



HAL
open science

Influence of non-equilibrium and nonlinear sorption of ^{137}Cs in soils. Study with stirred flow-through reactor experiments and quantification with a nonlinear equilibrium-kinetic model

Hamza Chaif, Arnaud Martin-Garin, Sylvie Pierrisnard, Daniel Orjollet,
Vanessa Tormos, Laurent Garcia-Sanchez

► To cite this version:

Hamza Chaif, Arnaud Martin-Garin, Sylvie Pierrisnard, Daniel Orjollet, Vanessa Tormos, et al.. Influence of non-equilibrium and nonlinear sorption of ^{137}Cs in soils. Study with stirred flow-through reactor experiments and quantification with a nonlinear equilibrium-kinetic model. *Journal of Environmental Radioactivity*, 2023, 257, pp.107067. 10.1016/j.jenvrad.2022.107067 . hal-03932717

HAL Id: hal-03932717

<https://hal.science/hal-03932717v1>

Submitted on 3 Feb 2023

HAL is a multi-disciplinary open access archive for the deposit and dissemination of scientific research documents, whether they are published or not. The documents may come from teaching and research institutions in France or abroad, or from public or private research centers.

L'archive ouverte pluridisciplinaire **HAL**, est destinée au dépôt et à la diffusion de documents scientifiques de niveau recherche, publiés ou non, émanant des établissements d'enseignement et de recherche français ou étrangers, des laboratoires publics ou privés.



Distributed under a Creative Commons Attribution - NonCommercial - NoDerivatives 4.0 International License

1 **Influence of non-equilibrium and nonlinear sorption of ^{137}Cs in soils.**
2 **Study with stirred flow-through reactor experiments and quantification**
3 **with a nonlinear equilibrium-kinetic model.**

4
5 Hamza Chaif^(a), Arnaud Martin-Garin^(a), Sylvie Pierrisnard^(a), Daniel Orjollet^(a), Vanessa
6 Tormos ^(a) and Laurent Garcia-Sanchez^{(a)*}

7 ^(a) : *Institute of Radiological Protection and Nuclear Safety (IRSN), Laboratory of*
8 *Research on Radionuclide Transfers in Terrestrial Ecosystems (LR2T), CE Cadarache,*
9 *13115, Saint-Paul-lez-Durance Cedex, France.*

10 * Corresponding author: laurent.garcia-sanchez@irsn.fr

11 **ABSTRACT**

12 This paper addresses the modelling of cesium sorption in non-equilibrium and nonlinear
13 conditions with a two-site model. Compared to the classical K_d approach, the proposed model
14 better reproduced the breakthrough curves observed during continuous-flow stirred tank
15 reactor experiments conducted on two contrasted soils. Fitted parameters suggested contrasted
16 conditions of cesium sorption between 1) equilibrium sites, with low affinity and high
17 sorption capacity comparable to CEC and 2) non-equilibrium sites, with a fast sorption rate
18 (half-time of 0.2-0.3 hours), a slow desorption rate (half-time of 3-9 days) and a very low
19 sorption capacity (0.02-0.04% of CEC). Comparison of EK sites densities with sorption
20 capacities derived from the literature suggests that the EK equilibrium and kinetic sites might
21 correspond to ion exchange and surface complexation of soil clay minerals respectively. This
22 work stresses the limits of the K_d model to predict ^{137}Cs sorption in reactive transport
23 conditions and supports an alternative non-equilibrium nonlinear approach.

24

25 **KEYWORDS**

26 cesium; sorption; soil; modelling; experiment; inverse modelling

27

28 **1. INTRODUCTION**

29 The various processes of solute retention on solid phases –referred to as *sorption* (Sposito,
30 1984)– strongly govern the mobility, bioavailability and remediation of substances in the
31 environment, and, in the case of radioactive substances, their radiological impact. They
32 notably control the conditions of reactive transport of solutes occurring in solid-liquid systems
33 such as rivers, soils and groundwater (Bouzidi et al., 2010; Fiengo Perez et al., 2015; Ilina et
34 al., 2020; Limousin et al., 2007). A critical issue when assessing the reactive transport of
35 solutes (such as radionuclides) in solid-liquid systems such as soils concerns the hypotheses
36 and parameters modelling the rate of solute transfer between the solution and solid phases
37 (Ardois and Szenknect, 2005; Chaif et al., 2021; Cherif et al., 2017; Limousin et al., 2007).

38 In impact assessment models, sorption is most commonly represented for a wide range of
39 contaminants (including radionuclides) by an instantaneous, concentration-independent and
40 completely reversible reaction, using an equilibrium coefficient also called distribution
41 coefficient and noted K_d (IAEA, 2009). This model simply assumes a constant proportion (K_d)
42 between concentrations in sorbed and soluble phases and, as a result, a constant proportion
43 (called retardation factor) between water and solute fluxes (Bossew and Kirchner, 2004;
44 Mishra et al., 2018; Szenknect et al., 2003). However, the K_d sorption model is not fully
45 predictive. Deviations from its simplifying hypotheses have been reported for many solutes
46 (including pesticides, radionuclides and notably cesium-137) and may result notably in earlier

47 solute arrival in groundwater and longer residence time in soils than the ideal K_d model (Bahr
48 and Rubin, 1987; Schnaar and Brusseau, 2014). These deviations essentially result from:

49 1) Chemical non-equilibrium: sorption sites may differ in their reactivity with the solute,
50 some reacting instantaneously and other slower than contact times with water (Chaif et al.,
51 2021; Kurikami et al., 2017; Ota et al., 2016; Sardin et al., 1991). Important special cases are
52 sorption irreversibility or pseudo-irreversibility: for a fraction of adsorbed solutes, the
53 remobilization back into solution may be impossible or so slow that it can be considered as
54 irreversible (Antonopoulos-Domis et al., 1995; Comans and Hockley, 1992; Montes et al.,
55 2013; Toso and Velasco, 2001).

56 2) Physical non-equilibrium: some sorption sites may not be instantaneously accessible to
57 the solute but limited by physical processes such as external and internal diffusion in solid
58 particles (Chen et al., 2020; van Genuchten and Wagenet, 1989).

59 3) Sorption nonlinearity: sorption may vary with solute concentration if it involves
60 multiple sorption sites having different densities and affinities for solute. For instance,
61 sorption can be high at trace levels when selective sorption sites are concerned, and much
62 lower when non-selective sorption sites also participate to solid-liquid exchanges (Cherif et
63 al., 2017; Fesch et al., 1998; Wang et al., 1998).

64 For a better description of sorption, various multi-site equilibrium and/or kinetic (EK)
65 models have been proposed. These empirical models, initially introduced for agrochemicals
66 and heavy metals (Cameron and Klute, 1977; Selim and Mansell, 1976; van Genuchten and
67 Wagenet, 1989), mitigate the K_d hypotheses by assuming that sorption occurs on 2–3 different
68 types of solid sites, governed by equilibrium and/or kinetic rates. Depending on the modelled
69 solutes, the existing variants combine multiple sorption properties such as equilibrium (e.g.
70 linear isotherm), non-equilibrium (first order, second order sorption rates), non-linearity (e.g.

71 Langmuir, Freundlich isotherms) and sorption irreversibility. More recently, promising
72 applications of EK models for radionuclide have been reported (Antonopoulos-Domis et al.,
73 1995; Chaif et al., 2021; Garcia-Sanchez et al., 2014; Ota et al., 2016; Toso and Velasco,
74 2001; Wang et al., 1998). However, the benefits of adopting equilibrium kinetic models of
75 sorption have not been fully demonstrated. The process-based validation of these approaches
76 still requires the interpretation of the different types of sorption sites in terms of real
77 contamination pools and not hidden virtual compartments. Moreover, the scenarios of reactive
78 transport for which EK hypotheses significantly improve the realism of predictions, compared
79 to the simple K_d hypotheses, must be clarified.

80 Sorption reactions in soils have been studied both in the laboratory and in the field by
81 complementary **experimental devices** that achieve different levels of representativity and
82 bring different levels of information **about sorption reactions**. They usually consist in **batch**
83 **experiments that allow a static study of sorption reactions in solid suspensions, or soil column**
84 **experiments that allow the study of reactive transport in porous media**.

85 **An intermediate experimental device known as *stirred flow-through reactor experiments*,**
86 **or continuous-flow stirred-tank reactor (CSTR) experiments, is particularly adapted to the**
87 **study of rate-limited sorption under flowing conditions in disperse solid phases. This device**
88 **consists in a well-mixed stirred cell, containing a known mass of solid and a known volume of**
89 **solution (e.g. Garcia-Sanchez et al., 2014; Martin-Garin et al., 2003; Sparks et al., 1980; Van**
90 **Cappellen and Qiu, 1997a,b) (Figure 1). During a classical reactor experiment, the injection**
91 **flowrate is generally held constant (Q_i) and the injected solute concentration consists in a**
92 **finite step function (with value C_i), while the dissolved concentration (C_w) is monitored at the**
93 **reactor outlet (Figure 2). Different reactor conditions allow then to test experimentally if**
94 **solute reactions depend on solute-concentration (C_i) and flowrate (Q), and are thus nonlinear**
95 **and not instantaneous (Bar-Tal et al., 1990).**

96 All these protocols require an inverse approach consisting in selecting a sorption model
97 and estimating its parameters from observations by frequentist or bayesian calibration (e.g.
98 Nicoulaud-Gouin et al., 2016; Toro and Padilla, 2017; van Genuchten et al., 2012). For model
99 selection, varying contact times and influent concentrations have been recommended to test
100 linearity and equilibrium hypotheses and reject improper models (e.g. Bar-Tal et al., 1990;
101 Nicoulaud-Gouin et al., 2016). For parameter identification, the unicity of the sorption
102 parameters derived from observations, also termed identifiability, must also be examined
103 attentively to ensure that obtained parameter values are physically interpretable (Belsley et al.,
104 1980; Brun et al., 2001; Stewart, 1987).

105 Large amounts of radionuclide have been released in the environment after the multiple
106 nuclear weapons tests that took place from the 1950s to 1980 and the nuclear accidents of
107 Chernobyl (1986) and Fukushima (2011) (Castrillejo et al., 2016; Klement, 1965; Steinhauser
108 et al., 2015). Among these elements, ^{137}Cs – due to its relatively long half-life ($t_{1/2} = 30.2$
109 years) – is considered the main source of radioactive soil contamination (Avery, 1996; Strebl
110 et al., 1999) and the first source of nuclear waste in the first one hundred years after release.

111 Cesium sorption in soils is primarily governed by clay minerals (Bostick et al., 2002;
112 Chorover et al., 2003; Missana et al., 2014a; Savoye et al., 2012; Shenber and Eriksson, 1993;
113 Wendling et al., 2005). In fact, radiocesium sorbs strongly and specifically on clay minerals
114 (Cornell, 1993; Fuller et al., 2015; Okumura et al., 2019) but also less intensely on iron oxides
115 and organic matter which often represent large sorption capacities (Rigol et al., 2002;
116 Schwertmann and Taylor, 1989). On clay minerals, surface adsorption sites are very
117 heterogeneous (Bradbury and Baeyens, 2000; Cornell, 1993; Eliason, 1966; Missana et al.,
118 2004; Poinssot et al., 1999; Staunton and Roubaud, 1997; Wahlberg and Fishman, 1962). Five
119 types of sorption sites are generally distinguished: basal surface sites, edge sites, hydrated
120 interlayer sites, frayed edge sites (FES), and interlayer sites (Okumura et al., 2019). These

121 sites have contrasted densities and affinities to cesium. Hydrated interlayer, FES, and
122 interlayer sites (that can be grouped under the term “interlayer sites”) have strong affinity to
123 cesium but low density (Brouwer et al., 1983; Eberl, 1980; Francis and Brinkley, 1976;
124 Jackson, 1962; Maes and Cremers, 1986; Poinssot et al., 1999; Rich and Black, 1964;
125 Sawhney, 1972; Zachara et al., 2002). Planar sites have much lower affinity to cesium but
126 represent most of the cation exchange capacity “CEC” and correspond to the basal surface
127 and edge sites (Cornell, 1993; Rigol et al., 2002; Staunton and Roubaud, 1997; Zachara et al.,
128 2002). Numerous laboratory studies indicate that Cs sorption is both time-dependent and
129 concentration-dependent. Sorption experiments show that, although ^{137}Cs sorption is initially
130 rapid (minutes), it continues for months from non-selective to highly selective sorption sites
131 (Konoplev et al., 1997). Desorption experiments also indicate that desorption of ^{137}Cs is very
132 slow (e.g. ~ 2 years of half-life for Fukushima soils reported by Murota et al., 2016)
133 particularly on clay minerals (Durrant et al., 2018). Moreover, many sorption isotherms
134 indicate that affinity to cesium decrease when the concentration of soluble cesium (Cs^+) and
135 its competitors (mainly K^+) increase in solution (Cherif, 2017; Siroux, 2017).

136 This work aimed at studying the hypotheses of non-equilibrium and non-linearity of
137 cesium sorption in reactive transport conditions. Our specific objectives were to: (1) quantify
138 the influence of cesium concentration and water transit time on sorption, (2) propose a simple
139 sorption model taking into account these effects, (3) study the validity of this model and
140 estimate its parameters, (4) relate the model compartments and parameters to measurable soil
141 properties. For these purposes, flow-through reactor experiments were conducted on two
142 contrasted soils under different conditions of injection concentration and flow rate. A 5-
143 parameter equilibrium-kinetic model (EK5) including both sorption non-equilibrium and non-
144 linearity was proposed to model cesium sorption and compared to a classical K_d approach. A

145 nonlinear regression approach was adopted to estimate K_d and EK5 parameters and to test
146 EK5 vs K_d hypotheses.

147 **2. MATERIAL AND METHODS**

148 **2.1. Studied Soils**

149 Two soils, noted “Soil H” and “Soil S”, were selected for their contrasted physico-
150 chemical and mineralogical properties (**Table 1**). Soil S was a calcareous sandy soil with pH
151 = 9.32, 1.44‰ of organic matter, and CEC= 1.11 cmol⁺/kg. Soil H, on the other hand, had a
152 loamy texture with pH = 5.5, 49.4‰ of organic matter, and CEC = 7.64 cmol⁺/kg. Soil
153 samples were air dried and sieved (<2 mm) before use. For soil S, mineralogy of the fraction
154 below 2µm was determined by ERM laboratory (Poitiers, France) using powder X-ray
155 diffractometer (Bruker D8 Advance A25) with CuKα radiation at 40kV and 40 mA on
156 oriented mounts. The same technique was used for soil H and the results were already
157 published in a previous study (Siroux, 2017; Siroux et al., 2021). The detailed mineral
158 composition of soils H and S is given in **Table S1** (in supplementary materials).

159

161 **Table 1.** Physico-chemical and mineralogical characteristics of soils H and S. Clay, silt and
 162 sand percentages correspond to the granulometric classes of the international scale. Illite,
 163 montmorillonite and kaolinite percentages correspond to mineralogical composition of the
 164 fraction of the soils below 2 μm , as determined by the X-Ray Diffractometry (XRD)
 165 technique. Percentage intervals correspond to the range of realistic mineralogical
 166 compositions compatible with the analytical results.

	Soil H*	Soil S
Clay (%)	13.13	3.10
Silt (%)	54.05	0.70
Sand (%)	32.82	96.20
pH (H ₂ O)	5.5	9.3
Organic matter (g/kg)	49.40	1.44
N (g/kg)	2.64	0.04
CaCO ₃ (g/kg)	14	118
Exchangeable cations (cmol+/kg)		
CEC	7.64	1.11
CEC <2 μm	20.0	18.7
K ⁺	0.32	0.23
Na ⁺	0.20	0.14
Ca ²⁺	3.23	31.20
Mg ²⁺	0.60	0.72
Mineralogy		
Illite (%)	11 - 22	0 - 2

Montmorillonite (%)	43 - 56	23 - 27
Kaolinite (%)	14 - 23	4 - 9

167

* data from Siroux (2017)

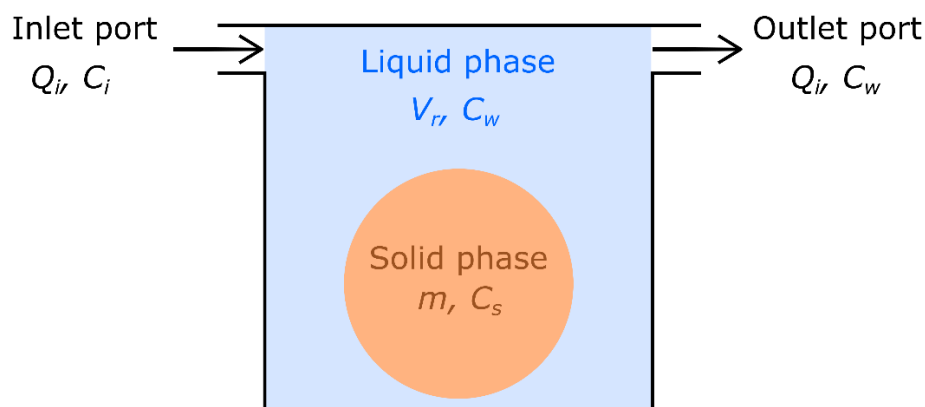
168

169

170 2.2. Stirred flow-through reactor experiments

171 Principles of continuous-flow stirred tank reactor experiments are presented in
172 introduction. Each experiment consisted in injecting an input solution into a chamber of
173 volume V_r containing a known mass of soil m , and measuring ^{137}Cs concentration (C_w) at the
174 output port of the chamber (Garcia-Sanchez et al., 2014; Martin-Garin et al., 2003; Van
175 Cappellen and Qiu, 1997a,b) (**Figure 1**). The input and output ports were equipped with 0.45
176 μm pore size hydrofoil Teflon membranes (HVLP, Millipore). The input solution was injected
177 at a constant flow rate in the reactor cell by a chromatography system (ÄKTATM pure 25), and
178 the direction of the flow was periodically reversed to avoid filter clogging. The continuous
179 stirring was ensured by attaching the reactor to an external shaker. This method was preferred
180 to a magnetic stir bar inside the cell to avoid destroying the solid particles. Samples were
181 collected using a fraction collector and analyzed for ^{137}Cs activity using a pure germanium
182 gamma spectrometer (Camberra EGPC 42.190.R).

183



184

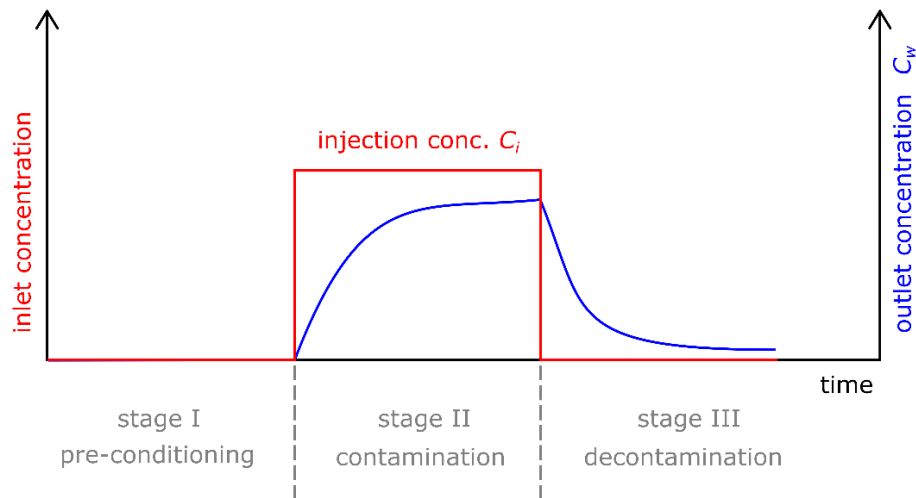
185 **Figure 1.** Principle of the continuous-flow stirred tank reactor (CSTR) experiments conducted
186 in this study. A solution is injected into the reactor chamber (of volume V_r) by its inlet port.

187 The solution is injected at a constant flow rate Q_i and is only contaminated during
188 contamination stage (with concentration C_i). Contaminant dilutes and interacts with the solid
189 phase (with mass m and contamination concentration C_s) inside the chamber. The reactor
190 chamber is well-mixed and has a homogenous contaminant concentration in solution C_w that
191 is monitored at the outlet port.

192

193 Each experiment consisted in a constant injection flow rate with three stages of
194 contaminant injection (**Figure 2**): (1) a pre-contamination stage (noted stage I) during which a
195 cesium-free solution was injected for at least 48 hours to allow the soil particles to reach a
196 chemical equilibrium with the input solution; (2) A contamination stage (noted stage II),
197 during which a cesium solution at a known concentration (C_i) was injected until the
198 normalized cesium concentration C_w/C_i either stabilized or reached 1; (3) A decontamination
199 stage (noted stage III) during which the cesium-free solution was again injected until the
200 normalized cesium concentration (C_w/C_i) was below 4%.

201



202

203 **Figure 2.** The three stages of continuous-flow stirred tank reactor (CSTR) experiments
204 conducted in this study. During each experiment, input solution was injected at a constant
205 flow rate Q_i (mL h^{-1}). During pre-conditioning (I) and decontamination (III) stages, input
206 solution was a cesium-free solution. During contamination (II), input solution had a constant
207 cesium concentration C_i (mol L^{-1}).

208

209 **2.3. Input solutions**

210 Cesium-free input solutions (**Table 2**) were designed to mimic the soil solution in
211 equilibrium with the soil. They were injected during the stages I and III of the experiments.
212 For soil S, Ultrapure water ($18 \text{ M}\Omega$ resistivity) was equilibrated with excessive amounts of
213 calcite (CaCO_3) and agitated in an open recipient to allow equilibrium with ambient air for at
214 least 15 days. The solution was then filtered and spiked with sodium chloride. For soil H,
215 Ultrapure pure water was directly spiked by a mixture of sodium chloride (NaCl), calcium
216 chloride (CaCl_2), calcium nitrate ($\text{Ca}(\text{NO}_3)_2$) and potassium chloride (KCl).

217 Cesium input solutions were prepared by spiking cesium-free input solutions with
218 approximate cesium concentrations of 10^{-3} mol L⁻¹, 10^{-5} mol L⁻¹, and 10^{-8} mol L⁻¹ depending
219 on the experiments (**Table 3**). These contaminated solutions were injected during the stages II
220 of the experiments. This spiking was achieved by adding a mixture of stable (CsCl) and
221 radioactive (¹³⁷Cs) cesium and then solution pH was adjusted (to pH=8.3 and 5.1 for soils S
222 and H, respectively) by adding a sodium hydroxide solution (NaOH). All cesium input
223 solutions contained approximately 500 Bq mL⁻¹ of ¹³⁷Cs.

224

225 **Table 2.** Composition of the input solutions used for the stirred flow-through reactor
226 experiments with the soils S and H. All concentrations are presented in mol L⁻¹

Property	Soil S	Soil H
[Ca ²⁺]	5.00E-04	3.00E-04
[Na ⁺]	5.00E-03	1.40E-04
[Cl ⁻]	5.00E-03	3.43E-04
[NO ³⁻]	-	4.60E-04
[K ⁺]	-	6.30E-05
pH	8.3	5.1

227

228 2.4. Experimental design

229 In order to study the influence of non-equilibrium and non-linearity of cesium sorption,
230 four stirred flow-through reactor experiments were conducted, for each soil, under different
231 cesium input concentrations (C_i) and flowrate (Q_i) conditions (**Table 3**). In total, our
232 experimental design combined three levels of cesium concentrations (10^{-3} mol L⁻¹, 10^{-5} mol L⁻¹,
233 and 10^{-8} mol L⁻¹) and two levels of flowrates (10 ml h⁻¹ and 35 ml h⁻¹).

234

235 **Table 3.** Experimental conditions of the 4 stirred flow-through reactor experiments conducted
 236 for soils S and H. The name of each experimental condition (e.g. “S8-10”) indicates the
 237 combination of soil name (i.e. S or H), approximate cesium input concentration C_i (i.e. 10^{-3} ,
 238 10^{-5} or 10^{-8} mol L⁻¹) and approximate flowrate Q_i (i.e. 10 or 35 mL h⁻¹).

Properties	Experiments							
	S3-10	S5-35	S8-10	S8-35	H3-10	H5-35	H8-10	H8-35
Soil	S	S	S	S	H	H	H	H
Q_i Average flow rate (mL h ⁻¹)	10.62	33.48	9.66	34.38	9.72	34.02	9.36	31.98
C_i Cesium concentration (mol L ⁻¹)	9.97E-04	9.71E-06	6.57E-09	6.92E-09	1.04E-03	9.97E-06	1.21E-08	1.00E-08
T_i Stage II duration (h)	141	92	262	194	140	71	671	294
Stage III duration (h)	263	192	938	602	338	195	1967	992
Stages II+III duration (h)	404	284	1200	796	478	266	2638	1286
m Soil mass (g)	3.70	3.78	3.78	3.57	2.83	3.12	3.06	3.09
V_r Reactor water volume (mL)	33.5	33.5	33.5	33.5	33.5	33.5	33.5	33.5

239

240 2.5. Empirical model of cesium sorption in stirred flow-through reactors

241 The 5-parameter sorption model EK5 considered here is a generalized version of an
242 empirical **linear non-equilibrium sorption** EK model (Chaif et al., 2021; Garcia-Sanchez et al.,
243 2014; Nicoulaud-Gouin et al., 2016) that can include sorption nonlinearity (**Figure 3**). Sorbed
244 concentrations are distributed between ‘fast’ sites (C_{s1}) noted type-1 sites that are
245 instantaneously in equilibrium with the aqueous phase –with an equilibrium constant noted
246 K_{d1} (L kg⁻¹)– and ‘slow’ sites (C_{s2}) noted type-2 sites that are governed by kinetic first order
247 mass transfer –with sorption and desorption rates noted k^+ (L kg⁻¹ s⁻¹) and k^- (s⁻¹) –. Type-1
248 and type-2 sites are supposed to have maximum sorption capacities C_{s1}^{max} (mol kg⁻¹) and
249 C_{s2}^{max} (mol kg⁻¹), **as supported by experimental Cesium isotherms (e.g. Cherif et al., 2017 ;**
250 **Siroux et al., 2021),** and their sorbed concentrations are modelled by a Langmuir isotherm and
251 a Langmuir kinetic equation (e.g. Selim et al., 1976; Fukui, 1978):

$$252 \quad C_{s1} = \frac{K_{d1}}{1 + \frac{K_{d1}}{C_{s1}^{max}} C_w} C_w \quad (1)$$

$$253 \quad \frac{dC_{s2}}{dt} = k^+ \left(1 - \frac{C_{s2}}{C_{s2}^{max}}\right) C_w - k^- C_{s2} \quad (2)$$

254 The affinity to cesium is quantified by the solid/liquid concentration ratio at equilibrium in
255 the absence of saturation ($C_{s1} \ll C_{s1}^{max}$, $C_{s2} \ll C_{s2}^{max}$). For type-1 sites, it corresponds by
256 definition to the equilibrium constant K_{d1} . For type-2 sites, the solid/liquid concentration ratio
257 tends to the equilibrium constant K_{d2} (L kg⁻¹) defined by:

$$258 \quad K_{d2} = \frac{k^+}{k^-}$$

259 which thus defines their affinity to cesium.

260 This general formulation contains 3 model variants, noted K_d , EK3 and EK5, relying on
 261 embedded hypotheses about type-1 and type-2 sorption sites (**Table 4**). The equations (1) and
 262 (2) of EK5 model encompass the 3-parameter linear EK model (noted EK3), which
 263 corresponds to the particular case of infinite sorption capacities C_{s1}^{max} and C_{s2}^{max} . They also
 264 encompass the classical 1-parameter K_d approach, which only considers type-1 sites, and
 265 corresponds to the particular case where $k^+ = 0$ and $k^- = 0$ and infinite C_{s1}^{max} .

266 In a stirred flow-through reactor with solid-liquid exchanges governed by the EK5 model,
 267 conservation equations for the exchangeable stock S_{ex} (mol) in solution and on type-1 sites,
 268 and for the fixed stock S_{fix} (mol) on type-2 sites, are then given by:

$$269 \quad \frac{dS_{ex}}{dt} = -k^+ m \left(1 - \frac{C_{s2}}{C_{s2}^{max}}\right) C_w + k^- S_{fix} + Q_i [C_i \delta(t) - C_w] \quad (3)$$

$$270 \quad \frac{dS_{fix}}{dt} = k^+ m \left(1 - \frac{C_{s2}}{C_{s2}^{max}}\right) C_w - k^- S_{fix} \quad (4)$$

271 where C_w (mol L⁻¹) is the dissolved cesium concentration, Q_i (L s⁻¹) is the flowrate, $\delta(t)$ is
 272 equal to 1 during contamination stage II and 0 otherwise, m is the soil mass. Exchangeable
 273 (S_{ex}) and fixed (S_{fix}) stocks are related to sorbed concentrations as follows:

$$274 \quad S_{ex} = V_r C_w + m C_{s1} \quad (5)$$

$$275 \quad S_{fix} = m C_{s2} \quad (6)$$

276 The system of equations (3)-(6) was implemented within the R environment (R Core
 277 Team, 2021) and was solved with the initial conditions $C_w(0)=0$, $C_{s1}(0)=0$ and $C_{s2}(0)=0$. In the
 278 case of solid-liquid exchanges governed by the K_d approach, equations (3)-(6) result in the
 279 following analytical solution for the breakthrough curve $C_w(t)$:

$$280 \quad C_w(t) = C_i \left(1 - e^{-\frac{Q}{R V_r} t}\right) \quad \text{if } t \leq T_i \quad (7)$$

281 $C_w(t) = C_w(T_i)e^{-\frac{Q}{RV_r}(t-T_i)}$ if $t > T_i$ (8)

282 where the retardation factor R corresponds in this case to:

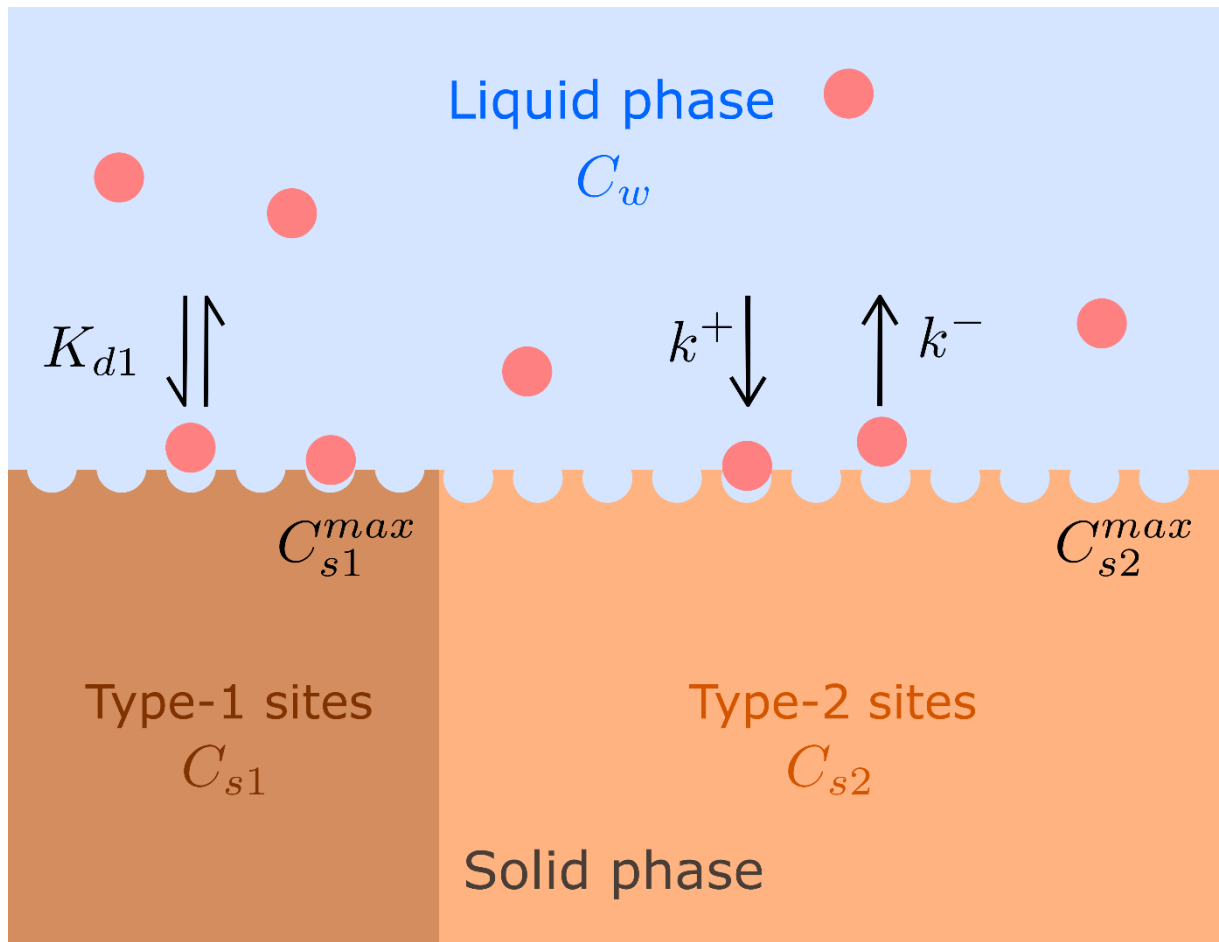
283 $R = 1 + \frac{m}{V_r}K_d$ (9)

284 In the general case, the system (3)-(6) was solved numerically with variable time steps by
285 an implicit finite-differences scheme. The implicit Radau IIA scheme, available in the R
286 package “deSolve” (Soetaert et al., 2010), was chosen for its stability, 5th order accuracy and
287 tolerance to stiff equations.

288 As a consequence of the mass-balance equations (3)-(4) above, half-times of sorption and
289 desorption reactions T^+ (s) and T^- (s) in a stirred flow-through reactor can be defined as
290 follows:

291 $T^+ = \frac{\log(2)V_r}{mk^+}$ (10)

292 $T^- = \frac{\log(2)}{k^-}$ (11)



293
294

295 **Figure 3.** Compartment representation of the 5-parameter Equilibrium-Kinetic model EK5
 296 applied to Cs sorption in this study. The model considers two types of solid sites for sorption.
 297 Type-1 sites are governed by equilibrium parameter K_{d1} ($L\ kg^{-1}$). Type-2 sites are controlled
 298 sorption by first-order sorption and desorption constants k^+ ($L\ kg^{-1}\ s^{-1}$) and k^- (s^{-1}). C_{s1}^{max} (mol
 299 kg^{-1}) and C_{s2}^{max} ($mol\ kg^{-1}$) denote the sorption capacities of type-1 and type-2 sites.
 300 Contaminant concentrations are denoted C_w ($mol\ L^{-1}$) in water, and C_{s1} , C_{s2} ($mol\ kg^{-1}$) in the
 301 solid phase.

302

303 **Table 4.** Parameters and hypotheses of the model variants K_d , EK3 and EK5 tested in this
 304 study to model Cesium sorption. These 3 special formulations derive from equations (1) and
 305 (2). EK5 corresponds to the full model, whereas K_d and EK3 introduce additional hypotheses
 306 about sorption (the absence of nonlinearity and non-equilibrium) that numerically correspond
 307 to particular fixed values for the sorption parameters k^+ , k^- , C_{s1}^{max} and C_{s2}^{max} .

Model variant	Sorption hypotheses	Free parameters	Fixed parameters
K_d	Linear equilibrium (type-1)	K_{d1}	$k^+ = 0, k^- = 0$ $C_{s1}^{max} = \infty$
EK3	Linear equilibrium (type-1)+ Linear non-equilibrium (type-2)	K_{d1}, k^+, k^-	$C_{s1}^{max} = C_{s2}^{max} = \infty$
EK5	Nonlinear equilibrium (type-1) + Nonlinear non-equilibrium (type-2)	$K_{d1}, k^+, k^-, C_{s1}^{max}$ C_{s2}^{max}	-

308

309 2.6. Estimation of sorbed cesium stocks

310 Sorbed cesium stocks Q_s (mol) were estimated at the end of contamination and
 311 decontamination stages II and III of each experiment in order to quantify cesium retention for
 312 the different experimental conditions. Calculations were derived from a mass-balance
 313 approach, and were based on the surface area separating breakthrough curves of cesium $C(t)$
 314 and of an inert tracer $C^{tr}(t)$ submitted to the same experimental conditions (Limousin et al.,
 315 2007; Martin-Garin et al., 2003). At any time t during the experiment, the sorbed cesium stock
 316 Q_s (mol) is governed by:

$$317 \quad Q_s(t) = V_r (C^{tr}(t) - C(t)) + \int_0^t Q(C^{tr}(\tau) - C(\tau)) d\tau \quad (12)$$

318 This formula was solved by numerical integration with the experimental concentrations
 319 $C_w(t)$ for cesium (eq. 3) and the analytical solution $C^{tr}(t)$ for the inert tracer, which is given
 320 by:

$$321 \quad C^{tr}(t) = C_i \left(1 - e^{-\frac{Q}{V_r} t}\right) \quad \text{if } t \leq T_i \quad (13)$$

322
$$C^{tr}(t) = C^{tr}(T_i)e^{-\frac{Q}{V_r}(t-T_i)} \quad \text{if } t > T_i \quad (14)$$

323 with the convention that $t=0$ at the beginning of contamination stage II.

324 In equation (12), C_w/C_i values that were superior to 1 during stage II (and have no physical
325 significance) were considered to be equal to 1 in order to avoid the underestimation of sorbed
326 stocks.

327

328 **2.7. Model calibration and local identifiability**

329 Sorption parameters of models K_d , EK3 and EK5 were estimated by the least squares method,
330 similarly to *in situ* calibrations detailed by Chaif et al. (2021). Briefly, the normalized
331 dissolved concentration $y_j=C_w/C_i$ was chosen as the observed variable in order to balance the
332 weight of each experiment. To ensure the convergence to an absolute optimum, the sum of
333 squares was minimized numerically from ten starting points by using the R routine “*optim*” (R
334 Core Team, 2021). These starting points had the least sum of squares among a large set of
335 candidate points evaluated in the parameters space (1000 for K_d model, 12^3 for EK3 model,
336 and 12^5 for EK5 model). The likelihood ratio statistic (LR) was used to test hypotheses about
337 sorption models (e.g. K_d vs EK3) (Huet et al., 2004). Confidence regions of estimated Cs
338 sorption parameters $\hat{\vartheta}$ for K_d , EK3 and EK5 models were approximated, at the level $100*(1 -$
339 $\alpha)\%$, by the points in the parameters space satisfying the Beale’s condition (Beale, 1960;
340 Seber and Wild, 1989). For each individual parameter $\hat{\vartheta}_i$, conservative confidence intervals
341 were then defined as the upper/lower bounds for ϑ_i in this region.

342 Identifiability, i.e. the unicity of the solution to the inverse problem, was diagnosed by the
343 conditioning number κ of the sensitivity matrix (Belsley et al., 1980; Brun et al., 2001;
344 Stewart, 1987), as fully described for reactor experiments by Nicoulaud-Gouin et al. (2016).

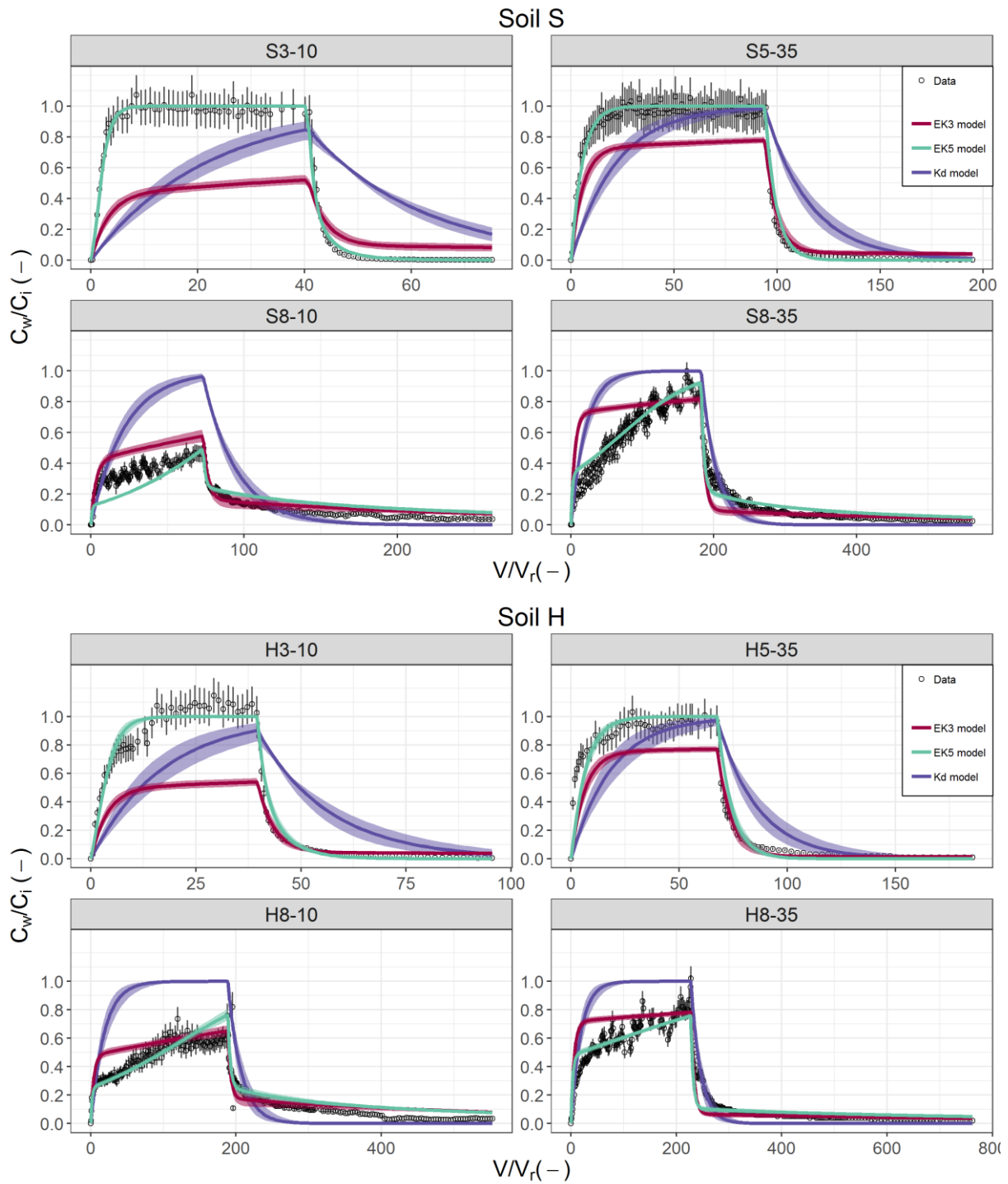
345 Conditioning numbers κ above 5 (resp. 10) were interpreted as moderately (resp. strongly)

346 non identifiable parameters (Belsley et al., 1980).

347

348 **3. RESULTS**

349 **3.1 Experimental breakthrough curves**



354 Dots correspond to observations and color lines correspond to least squares fits with the K_d
355 (purple), EK3 (red) and EK5 (green) models. Vertical bars correspond to the confidence
356 intervals of the observations. Purple, red, and green shaded bands correspond to the 95%
357 parametric uncertainty of fitted curves.

358

359 For both soils, our observations evidenced influences of flowrate and input concentrations
360 on cesium sorption and thus support the non-equilibrium and nonlinear hypotheses (**Figure**
361 **4**).

362 Cesium outlet concentrations C_w/C_i during contamination stage II systematically increased
363 with flowrate. For instance, the input concentration was completely transmitted to the outlet
364 ($C_w/C_i = 1$) after a cumulated flowed volume V of around 200 reactor volumes (V_r) at 35 mL
365 h^{-1} (experiments S8-35 and H8-35), whereas the breakthrough was still incomplete at 10 mL
366 h^{-1} at the end of contamination stage II (C_w/C_i below 0.6 for experiments S8-10 and H8-10).
367 This trend indicates a smaller sorption when contact time with cesium decreases. These
368 observations prove the influence of non-equilibrium in cesium sorption processes for the
369 studied soils.

370 Cesium outlet concentrations C_w/C_i during contamination stage II systematically increased
371 when input concentration increased. For high input concentrations (10^{-3} mol L^{-1}), the
372 equilibrium state, corresponding to $C_w/C_i = 1$, was reached after the injection of 10-25 reactor
373 volumes V_r (S3-10 and H3-10) whereas for low concentrations (10^{-8} mol L^{-1}) it was not
374 achieved even after 80-200 V_r ($C_w/C_i = 0.46$ and $C_w/C_i = 0.63$ for S8-10 and H8-10
375 respectively). This trend indicates less soil capacity to fix cesium at higher dissolved
376 concentrations. These observations prove the influence of nonlinearity on cesium sorption
377 processes for the studied soils.

378 Cesium sorption was also affected by the nature of the soils. While similar input conditions
379 provided similar BTC shapes for both soils, some differences in the equilibrium time were
380 observed between the two soils. Convergence to equilibrium state was always faster for soil S
381 than for H. For instance, outlet concentration was stabilized after the injection of 30 V_r for S5-
382 35 compared to 50 V_r for H5-35.

383

384 **3.2. Sorbed concentrations and restitution**

385 Estimated sorbed stocks during contamination and decontamination stages II and III also
386 revealed influences of flowrate and input concentrations on the reversibility of cesium
387 sorption (**Table 5**).

388 Cesium desorption during decontamination stage III (termed here restitution) increased
389 with injection concentration and indicated more reversible processes. For high injection
390 concentration experiments (above 10^{-5} mol L⁻¹), restitution was always over 65% for both
391 soils. At low injection concentrations (10^{-8} mol L⁻¹), restitution did not exceed 50% and was
392 around 34% (S8-10) at low flowrate and reached around 47% at high flowrate (S8-35).

393 Cesium restitution also increased with flowrate. For instance, restitution was around 35%
394 for low flowrate experiments (S8-10 and H8-10) and reached around 45% with higher
395 flowrate (S8-35 and H8-35).

396

397 **Table 5.** Experimental and EK5 simulated stocks of Cs at the end of contamination and
 398 decontamination stages II and III as defined in equation (12). Restitution is defined at the ratio
 399 of the desorbed and sorbed stocks of Cs.

Conditions	Calculation	Stock at end of stage II (mol)	Stock at end of stage III (mol)	Restitution (%)
S3-10	Experiment	6.38E-05	2.51E-05	61
	EK5	7.13E-05	7.46E-08	100
S5-35	Experiment	2.17E-06	7.70E-07	64
	EK5	1.77E-06	1.43E-08	99
S8-10	Experiment	1.02E-08	6.74E-09	34
	EK5	1.16E-08	6.66E-09	43
S8-35	Experiment	1.62E-08	8.54E-09	47
	EK5	1.47E-08	5.33E-09	64
H3-10	Experiment	1.32E-04	4.28E-05	68
	EK5	1.32E-04	5.76E-08	100
H5-35	Experiment	2.15E-06	4.49E-08	98
	EK5	2.24E-06	4.82E-08	98
H8-10	Experiment	3.95E-08	2.63E-08	33
	EK5	3.88E-08	1.79E-08	54
H8-35	Experiment	2.92E-08	1.70E-08	42
	EK5	2.93E-08	1.69E-08	42

400

401 3.3. Cesium sorption modelling

402 For both soils, EK5 model described significantly better the observed non-equilibrium and
 403 nonlinear effects than EK3 and K_d models.

404 Qualitatively, the model EK5, with 5 degrees of freedom, better fitted the breakthrough
 405 curves than EK3 and K_d models (3 and 1 degrees of freedom) (**Figure 4**). With a constant
 406 retardation factor R (eq. 9) for all conditions, the K_d model underestimated C_w/C_i at high input
 407 concentration values and overestimated them at low concentration values ($C_w/C_i=1$ at the end
 408 of stage II of all experiments). With kinetic rates of sorption and desorption allowing
 409 asymmetry in the curves between stages II and III, EK3 model better fitted C_w/C_i during stage

410 III whereas it was still unrealistic during stage II (S5-35, H3-10, and H5-35 for example).
411 With sorption capacities potentially limiting the sorption on type-1 and type-2 sites, EK5
412 model better described the strong inflexions of C_w/C_i during stage II for all experiments with
413 two exceptions being S8-10 where sorption was slightly overestimated at the start of stage II,
414 and H8-10 where sorption was underestimated at the end of stage II.

415 Sorbed stocks predicted by the EK5 model showed two distinct behaviors depending on
416 the input concentrations (Table 5). At high concentrations, sorption was completely reversible
417 with restitution rates superior to 98% for both soils. At low concentrations, sorption was
418 irreversible and restitution never exceeded 64%. These results suggest that EK5 model can
419 reproduce both reversible and irreversible behaviors depending on the experimental
420 conditions using the same set of parameters.

421 Quantitatively, the better performance of EK5 model vs EK3 and K_d was confirmed
422 statistically for both soils by the likelihood ratio tests (Table 6). Even though the inclusion of
423 non-equilibrium sorption significantly improved the fit (EK3 vs K_d), the addition of nonlinear
424 sorption made it even better, as indicated by p-values always under 10^{-16} for the likelihood
425 ratio test of model EK3 vs model EK5. These results prove that the formulation of sorption
426 nonlinearity and non-equilibrium proposed by model EK5, although still very simple, brings a
427 significant improvement to EK3 and K_d alternatives and suggest its applicability to various
428 soils.

429

430 **Table 6.** Statistics summary of the fits of sorption models (K_d , EK3 and EK5). For each soil,
 431 sorption models were fitted simultaneously on the 4 stirred flow-through reactor experiments.
 432 Sum of squares S denotes the sum of squared errors between model predictions and
 433 observations. The p-value of the Likelihood ratio (LR) statistic was derived from its
 434 approximate chi-squared distribution, as detailed in Chaif et al. (2021).

Quantity		Soil S	Soil H
Sum of squares S	K_d model	65.4	51.7
	EK3 model	29.6	17.4
	EK5 model	3.50	4.43
K_d vs EK3	LR	665	786
	p-value	<1e-16	<1e-16
K_d vs EK5	LR	2455	1771
	p-value	<1e-16	<1e-16
EK3 vs EK5	LR	1790	985
	p-value	<1e-16	<1e-16

435

436 3.4 Fitted parameters

437 For both soils, fitted EK5 parameters suggested very contrasted conditions of cesium
 438 sorption between equilibrium and non-equilibrium sites in terms of characteristic sorption
 439 times, affinity and sorption capacity (**Table 7**).

440 The type-1 equilibrium sites had a very high sorption capacity, as indicated by C_{sl}^{max}
 441 values comparable to soil CEC (**Table 1**), but had a non-specific affinity to cesium, as
 442 indicated by low K_{d1} values (40 - 60 L kg⁻¹ depending on the soil).

443 The type-2 non-equilibrium sites had a fast sorption rate k^+ and a slow desorption rate k^- .
444 Sorption half-times T^+ of less than one hour for both soils (0.2 and 0.3 hours on average for
445 soils S and H respectively) were shorter than mean residence time of solution in the reactors
446 (0.96 to 3.35 hours depending on the flowrate) and indicated a fast cesium sorption.
447 Desorption half-times T^- were much longer (3 and 9 days on average for soils S and H
448 respectively) and suggested a pseudo-irreversible cesium sorption.

449 The type-2 non-equilibrium sites had a very strong affinity to cesium but with a very
450 limited sorption capacity. They had a specific affinity to cesium, as indicated by large values
451 of their theoretical equilibrium ratio $K_{d2} = k^+/k^-$ (3489 to 6171 L kg⁻¹ for soils S and H
452 respectively). Their sorption capacity C_{s2}^{\max} was very small (0.04% and 0.02% of the CEC of
453 soils S and H respectively) and indicated a very limited number of type-2 sites.

454 Soil H had a higher cesium sorption capacity than Soil S. Distribution coefficient of both
455 equilibrium and kinetic sites K_{d1} and K_{d2} were respectively 51% and 77% higher in soil H
456 than in S. Similarly, equilibrium and kinetics sites saturations C_{s1}^{\max} and C_{s2}^{\max} were 456%
457 and 260% higher in H than S. These values are in line with the contrasted physiochemical and
458 mineralogical properties of the two soils, notably the higher CEC and clay and organic matter
459 content of soil H compared to S (**Table 1**).

460

461 **Table 7.** Fitted parameter values of the EK5 model. Values correspond to ordinary least-
 462 squares estimations, and intervals correspond to conservative 95% confidence intervals.

Parameter	Unit	Soil S	Soil H
K_{d1}	$L\ kg^{-1}$	40 [34 ; 46]	60 [49 ; 74]
k^+	$L\ kg^{-1}\ s^{-1}$	4.71E-03 [4.27E-03 ; 5.24E-03]	2.45E-03 [2.20E-03 ; 2.73E-03]
k^-	s^{-1}	1.35E-06 [1.15E-06 ; 1.59E-06]	3.98E-07 [3.07E-07 ; 5.01E-07]
C_{s1}^{max}	$mol\ kg^{-1}$	1.38E-02 [1.01E-02 ; 1.92E-02]	7.67E-02 [4.94E-02 ; 1.39E-01]
C_{s2}^{max}	$mol\ kg^{-1}$	4.83E-06 [4.49E-06 ; 5.21E-06]	1.74E-05 [1.55E-05 ; 2.01E-05]

463

464 4. DISCUSSION

465 4.1. Experimental design

466 Our experimental design (combining 3 concentration levels and 2 flowrate levels in 4
467 experiments) allowed to identify uniquely and accurately the EK5 parameters for both soils.
468 The conditioning numbers κ (2.291 and 2.505) well below 5 indicated *a posteriori* that our
469 experimental design constrained the fitted equations (3)-(4) to a unique set of parameter
470 values (Table 8). The good identifiability of EK5 parameters was also confirmed numerically
471 by the narrow confidence intervals of parameters, whose half-width did not exceed 16% for
472 Soil S and 26% for Soil H (Table 7).

473 These numerical results suggest the adoption of our 4 reactor design for future CSTR
474 experiments aiming at identifying EK5 parameters for other soils/radionuclides. They are
475 complementary to more formal analyses recommending at least 2 experiments for the
476 identification of the EK3 model (Nicoulaud-Gouin et al., 2016).

477 Considering that EK5 model well fitted the BTC curves, the EK5 parameters obtained in
478 this study can be seen as simple but accurate indicators of sorption processes, and, as such,
479 deserve further discussion about their physical interpretation.

480

481 **Table 8.** Local identifiability of EK5 parameters for soils S and H, as diagnosed from the
482 conditioning number κ of the sensitivity matrix (Brun et al., 2001). The applied formulae are
483 fully detailed in Nicoulaud-Gouin et al. (2016).

	Notation	Soil S					Soil H				
Eigenvalues	λ_i	2.079	1.155	0.862	0.508	0.396	2.025	1.398	0.724	0.530	0.323
Conditioning number	κ	2.291					2.505				

485 4.2. Physical nature of type-1 and type-2 sites

486 Since cesium sorption in soils is primarily governed by clay minerals (Bostick et al., 2002;
487 Chorover et al., 2003; Missana et al., 2014a; Savoye et al., 2012; Shenber and Eriksson, 1993;
488 Wendling et al., 2005), it seems plausible that the equilibrium and kinetic sites postulated by
489 the EK5 model are an empirical typology of the various clay sorption sites.

490 The non-linearity of Cs sorption is mainly due to the heterogeneity of the surface
491 adsorption sites (Bradbury and Baeyens, 2000; Cornell, 1993; Eliason, 1966; Missana et al.,
492 2004; Poinssot et al., 1999; Staunton and Roubaud, 1997; Wahlberg and Fishman, 1962)
493 which, as reviewed in introduction, broadly includes interlayer sites with low density strong
494 affinity to cesium but and planar sites with higher densities but lower affinity cesium. These
495 observations have been summarized quantitatively with a simplified two-site thermodynamic
496 model of Cs sorption on clay noted 1-pK DL/IE (Cherif et al., 2017). The first sites are
497 governed by an ion exchange (IE) model which simulates the adsorption of Cs on negatively
498 charged sites of planar surface of clay minerals, including outer-basal and interlayers sites
499 ($\equiv X^-$). The second sites are governed by a surface complexation (SC) model used to describe
500 the adsorption of cations on a single FES site ($\equiv SO^{-0.5}$) (Cherif et al., 2017 and references
501 therein). A database of these sites densities is available for illite, montmorillonite and
502 kaolinite minerals. Therefore, for a given soil, knowing its mineralogical composition allows
503 the estimation of IE and surface complexation sites densities (Table 9).

504 The densities of type-1 equilibrium sites (given by C_{s1}^{\max}) and type-2 kinetic sites (given
505 by C_{s2}^{\max}) of EK5 model seem to correspond to those of IE and SC sites of clay minerals of
506 both soils respectively (Table 9). On one hand, IE sites densities were almost identical to
507 C_{s1}^{\max} for soil S (relative error of 5%) and around two times higher for soil H. On the other

508 hand, the offset between C_{s2}^{max} and surface complexation sites densities was of a similar
509 magnitude for both soils (relative error of 80% and 52% for S and H respectively). These
510 differences can be explained by : (1) the presence of other sites, mainly organic matter, that
511 can contribute to cesium sorption (Nakamaru et al., 2007; Rigol et al., 2002; Valcke and
512 Cremers, 1994); (2) The uncertainty related to the estimation of proportions of the clay
513 minerals (illite, montmorillonite and kaolinite available in the soils). In fact, the XRD method
514 used to estimate these proportions is semi-quantitative and only provides a gross estimation of
515 these proportions (Table 1).

516 With parameters values of C_{s1}^{max} and C_{s2}^{max} fixed to Exchange and surface complexation
517 sites densities of the studied soils (Table 9), the model EK5 yielded satisfactory predictions of
518 BTC (Figure 5). The model EK5 satisfactorily reproduced all the experimental breakthrough
519 curves except for experiments S8-10 and S8-35, where predicted concentrations C_w/C_i
520 increased towards unity earlier than observed. This is mainly due to the surface complexation
521 sites density being slightly lower than C_{s2}^{max} which lead to a premature saturation of kinetic
522 sites at the end of stage II of experiment S8-10. The exchange and surface complexation sites
523 densities seem to provide a good first indicator of the sorption capacities of equilibrium and
524 kinetic sites. However, the uncertainties associated with the proportions of minerals and their
525 IE and SC densities may explain the imprecise estimation of the C_{s1}^{max} and C_{s2}^{max} parameters.

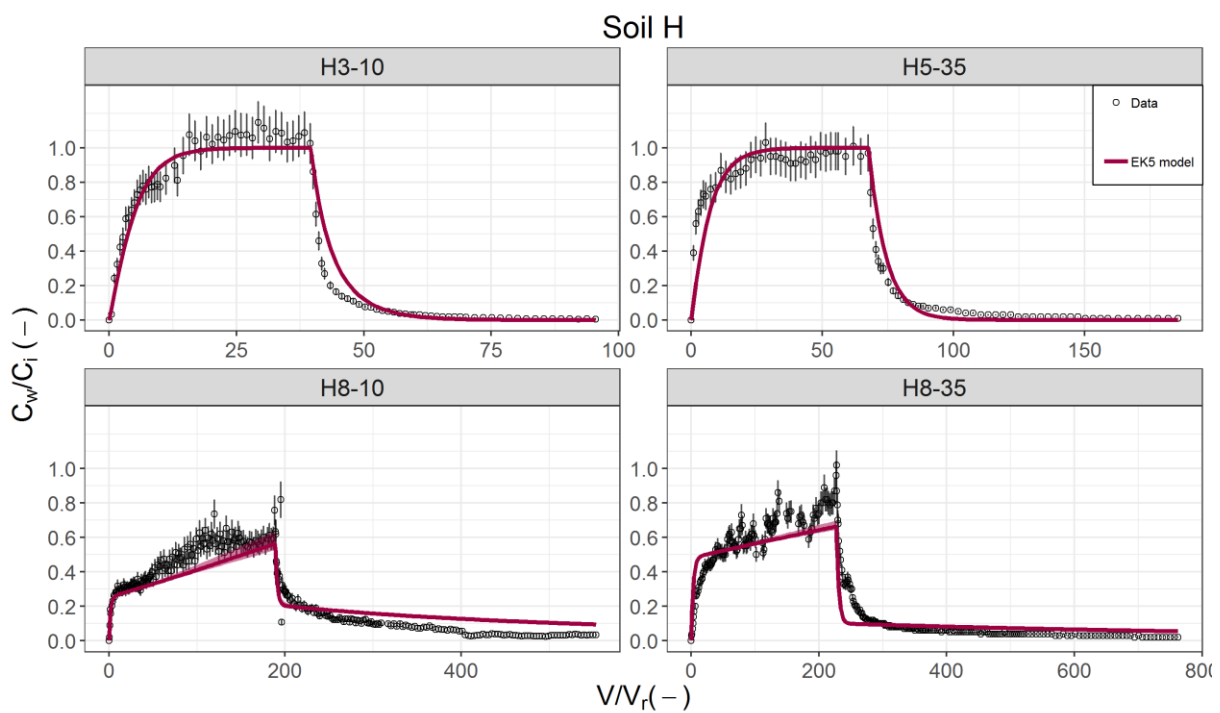
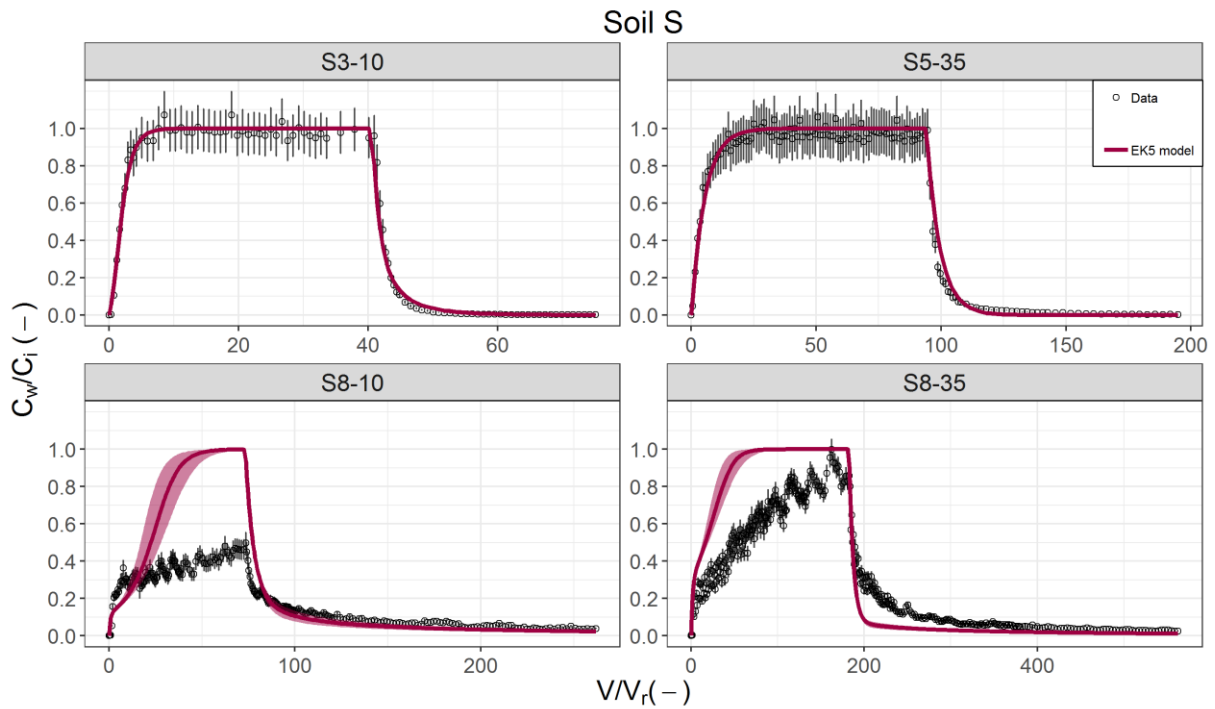
526

527 **Table 9.** Exchange and surface complexation sites densities derived from the mineralogical
 528 properties of the studied soils and the properties of illite, montmorillonite and kaolinite
 529 compiled by Cherif et al. (2017). Cation exchange capacity (CEC) (from **Table 1**) and fitted
 530 sorption capacities C_{s1}^{\max} and C_{s2}^{\max} (from **Table 7**) are recalled here to support the
 531 comparisons given in the text.

	Soil S			Soil H		
	Min	Mean	Max	Min	Mean	Max
Ion Exchange “IE” sites density (mol kg⁻¹)	1.19E-02	1.31E-02	1.43E-02	1.53E-01	1.80E-01	2.07E-01
CEC (mol kg⁻¹)	1.11E-02			7.64E-02		
C_{s1}^{\max} (mol kg⁻¹)	1.01E-02	1.38E-02	1.92E-02	4.94E-02	7.67E-02	1.39E-01
Surface complexation sites density (mol kg⁻¹)	6.59E-07	9.77E-07	1.30E-06	2.63E-05	3.66E-05	4.70E-05
C_{s2}^{\max} (mol kg⁻¹)	4.49E-06	4.83E-06	5.21E-06	1.55E-05	1.74E-05	2.01E-05

532

533



537 **Figure 5.** Cs breakthrough curves simulated by the EK5 model with C_{s1}^{\max} (resp. C_{s2}^{\max})
 538 equal to the ion exchange (resp. surface complexation) sites densities (**Table 9**). Other
 539 parameters (K_{d1} , k^+ , and k^-) were at fitted values (**Table 7**).

540 **4.3. Cesium sorption and reversibility on equilibrium and kinetic sites**

541 The EK5 hypothesis better reproduced the experimental results by considering that
542 sorption sites act differently at low, intermediate and high concentrations of cesium (**Figure**
543 **6**).

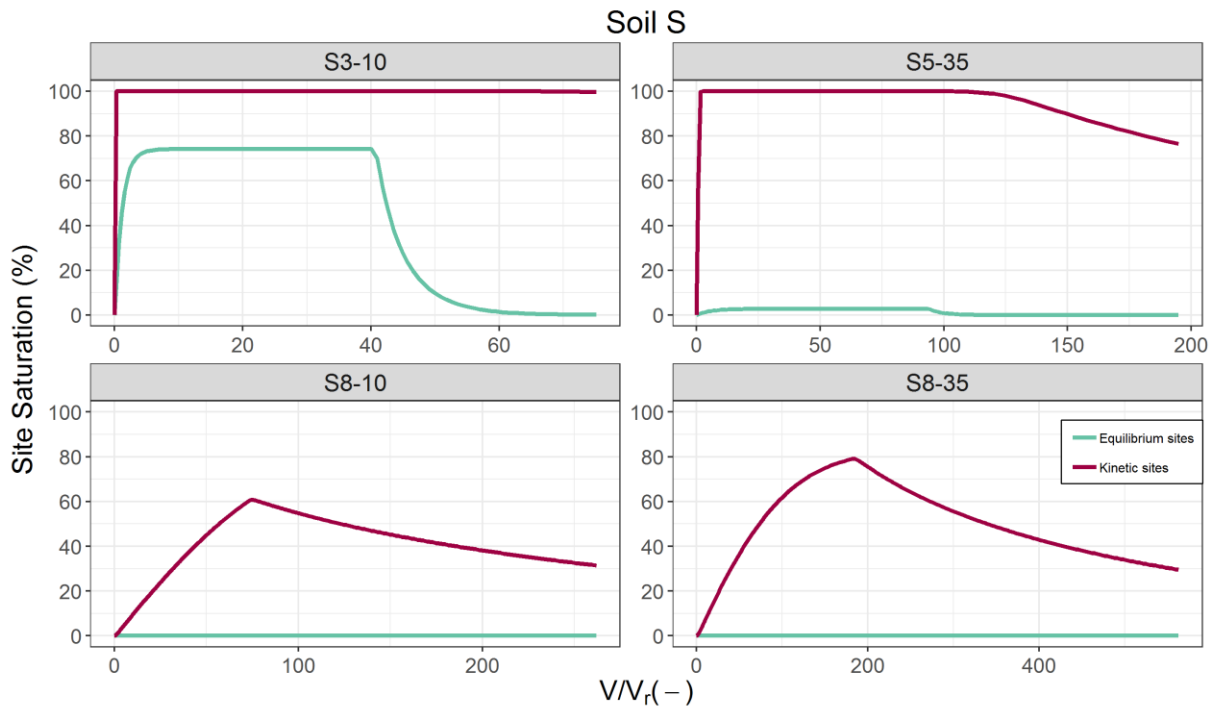
544 At low input concentrations (10^{-8} mol L⁻¹), simulated Cs sorbed on type-2 sites without
545 saturation of sorption capacity at the end of contamination stage II (e.g. 60% for S8-10 and
546 80% for S8-35). Simulated Cs sorption on type-1 sites was virtually inexistent (with
547 saturation index almost at 0%) due to their much lower affinity to Cs. As a consequence,
548 simulated Cs desorption during decontamination stage III resulted only from type-2 sites.

549 At high input concentrations (10^{-3} mol L⁻¹), simulated Cs also initially sorbed on type-2
550 sites. However, type-2 sites rapidly reached saturation (less than one hour), and simulated Cs
551 continued to sorb on type-1 sites without saturation at the end of contamination stage II (e.g.
552 around 75% for S3-10 and 45% H3-10). Considering that type-1 sites held almost all the
553 sorbed inventory, simulated Cs desorption during decontamination stage III resulted only
554 from type-1 sites.

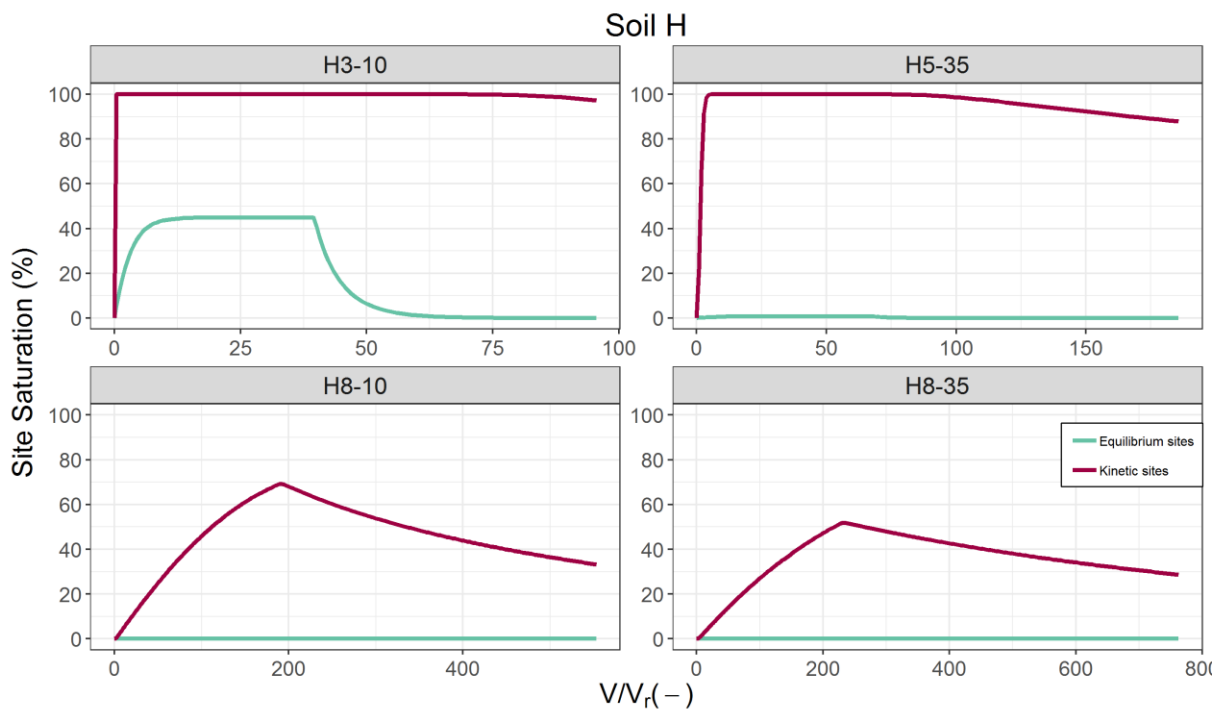
555 At intermediate input concentrations (10^{-5} mol L⁻¹), simulated Cs initially sorbed on type-2
556 sites (at short times) and on type-1 sites during contamination stage II. During
557 decontamination stage III, type-1 and type-2 sites both contributed to desorption in the
558 opposite order. Indeed, simulated Cs initially desorbed exclusively from low affinity type-1
559 sites. After type-1 sites were rapidly decontaminated (less than 6 hours), simulated Cs
560 continued to desorb from high affinity type-2 sites and this process was much slower.

561 This behavior of the EK5 model is consistent with studies evidencing specific and non-
562 specific cesium sorption in soils. In fact, several studies conducted on clay minerals (illite,

563 montmorillonite and kaolinite) have shown that cesium sorption takes place on two distinct
564 sites with different affinities (Benedicto et al., 2014; Brouwer et al., 1983; Missana et al.,
565 2014b; Poinssot et al., 1999; Staunton and Roubaud, 1997). The sorption isotherms obtained
566 in these studies showed that cesium sorption depended on the cesium concentration in the
567 solution. At low concentrations, cesium sorption was the highest and decreased when cesium
568 concentrations increased.



570



571

572 **Figure 5.** Percentage of occupied sites for type-1 equilibrium (green) and type-2 kinetic (red)
 573 sites, as simulated by the EK5 model with fitted parameters (Table 7). Cumulated flowed
 574 volume at the reactor outlet V is normalized by the volume V_r of the reactor chamber.

575 4.4. Domains of sorption nonlinearity and non-equilibrium

576 Rewriting the equations of reactive transport (3)-(4) can reveal when nonlinear and non-
 577 equilibrium effects are significant (and the full EK5 model is required) and when linearity or
 578 equilibrium hypotheses are appropriate (and K_d or EK3 models can be used).

579 In the case of the EK3 model, the reactive transport equations (3) and (4) have been
 580 rewritten in a simplified form by introducing the following transformations (Nicoulaud-Gouin
 581 et al., 2016):

$$C_w^* = \frac{C_w}{C_i}; \quad C_{s2}^* = \frac{m C_{s2}}{V_r C_i}; \quad t^* = \frac{Q_i t}{V_r}; \quad D_{a1} = \frac{m k^+}{Q_i}; \quad D_{a2} = \frac{V_r k^-}{Q_i}; \quad K_{d1}^* = \frac{m}{V_r} K_{d1}$$

582 where C_w^* and C_{s2}^* are dimensionless concentrations in solution and on type-2 sites, t^* is
 583 dimensionless time, D_{a1} and D_{a2} are ratios of sorption and desorption times to water residence
 584 time, also known as Damköhler numbers (Bahr and Rubin, 1987). In the case of the full EK5
 585 model, reactor equations (3) and (4) here write:

$$586 \quad \frac{dC_w^*}{dt^*} = -\frac{1+D_{a1}(1-\tau_2)}{R(C_w^*)} C_w^* + \frac{D_{a2}}{R(C_w^*)} C_{s2}^* + \frac{\delta}{R(C_w^*)} \quad (15)$$

$$587 \quad \frac{dC_{s2}^*}{dt^*} = D_{a1}(1-\tau_2)C_w^* - D_{a2}C_{s2}^* \quad (16)$$

$$588 \quad R(C_w^*) = 1 + \frac{K_{d1}^*}{\left(1 + \frac{K_{d1}^*}{C_{s1}^{max*}} C_w^*\right)^2} \quad (17)$$

589 where R is the retardation factor due to type-1 sites. The dimensionless sorption capacity
 590 C_{s1}^{max*} of type-1 sites and the rate of occupied type-2 sites τ_2 are defined by:

$$C_{s1}^{max*} = \frac{m C_{s1}^{max}}{V_r C_i}; \quad \tau_2 = \frac{C_{s2}}{C_{s2}^{max}}$$

591 In equation (15), type-2 sorption of a contaminant is significant if $D_{a1} > 1$, or equivalently
592 if the half-time of the sorption reaction T^+ is shorter than water residence time ($T^+ < T_w$).
593 Similarly, type-2 desorption of a contaminant can occur significantly if $D_{a2} > 1$, or
594 equivalently if the half-time of the desorption reaction T^- is shorter than water residence time
595 ($T^- < T_w$). As a consequence, the condition ($T_w < T^+$ or $T_w < T^-$) corresponds to the non-
596 equilibrium sorption domain, and in particular, the domain $T_w \ll T^-$ corresponds to pseudo-
597 irreversible sorption (**Figure 7**).

598 Type-1 sorption is governed by a Langmuir isotherm (eq. 1) and tends to saturate when
599 $K_{d1}C_w/C_{s1}^{\max}$ exceeds 1, which corresponds to C_w greater than C_{s1}^{\max}/K_{d1} . Quantitatively,
600 type-1 sites are saturated at 50% when C_w is equal to C_{s1}^{\max}/K_{d1} , and are saturated at 99%
601 when C_w is approximately $100 C_{s1}^{\max}/K_{d1}$. Similarly, from equation (2), type-2 sorption tends
602 at equilibrium to a Langmuir isotherm, which saturates when C_w is greater than C_{s2}^{\max}/K_{d2} .
603 As a consequence, dissolved cesium concentrations C_w lying in the intervals
604 $[1,100]*C_{s1}^{\max}/K_{d1}$ or $[1,100]*C_{s2}^{\max}/K_{d2}$ correspond to the domain of nonlinear sorption
605 (**Figure 7**).

606 This analysis thus shows that the minimal sorption model depends on the residence time of
607 water (T_w) and the dissolved cesium concentration in water (C_w). Three broad sorption
608 domains can be defined and distinguished in the plane (T_w, C_w) (**Figure 7**): the equilibrium
609 domain (where sorption can be described by an isotherm model, including the K_d model at
610 trace concentrations), the linear equilibrium (where the linear kinetic approximation EK3
611 applies) and the nonlinear non-equilibrium domain (where the full EK5 cannot be simplified).
612 The nonlinear non-equilibrium domain indicates the reactive transport scenarios for which the
613 EK5 model can improve the realism of predictions.

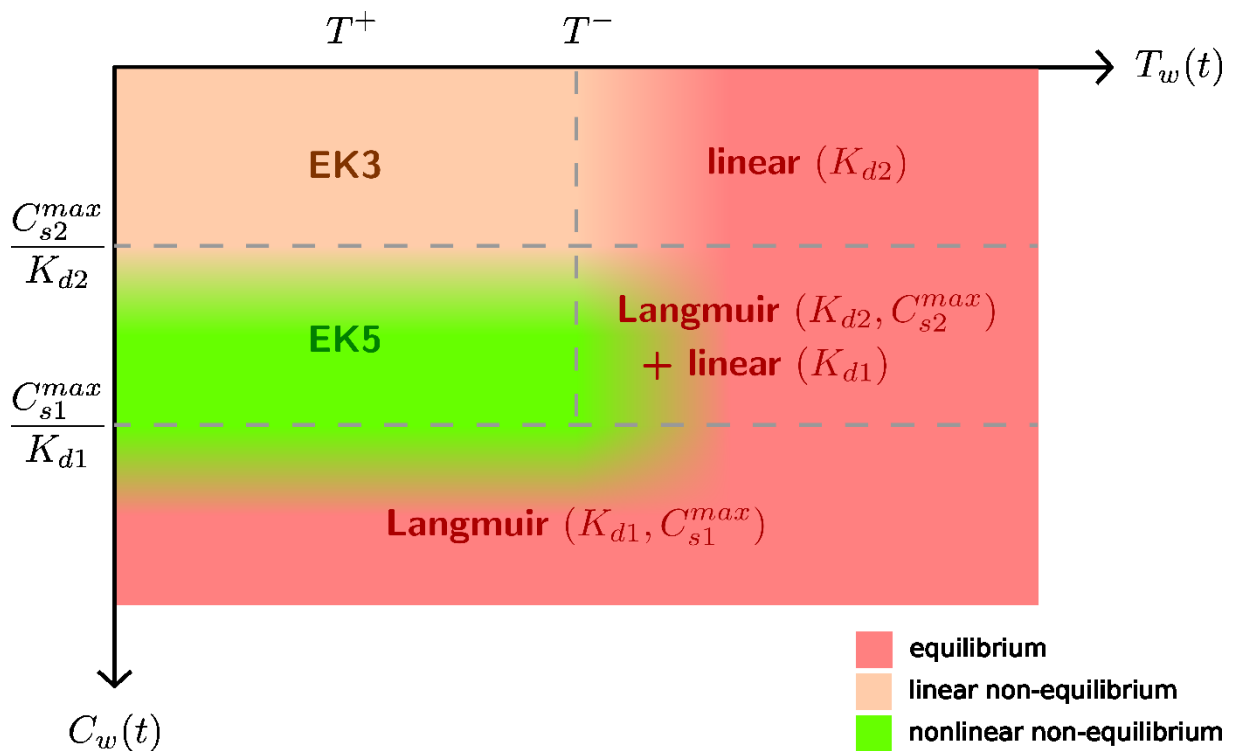
614 For scenarios of radiocesium release in the environment, the influence of sorption
615 nonlinearity may not be significant on reactive transport and the approximations of models K_d
616 or EK3 may be valid. Indeed, the linear domain corresponds to dissolved concentrations
617 below C_{s2}^{\max}/K_{d2} , i.e. approximately below $1.4 \cdot 10^{-9}$ and $2.8 \cdot 10^{-9}$ mol L⁻¹ for the studied soils S
618 and H. In the case of ¹³⁷Cs (with mass activity $3.22 \cdot 10^{12}$ Bq g⁻¹), this would correspond to
619 maximum concentrations of 71 and 146 kBq L⁻¹. However, nonlinear sorption may occur at
620 much lower concentrations C_w in the presence of stable cesium in the soil and more
621 competing cations in the solution (e.g. Fukui, 1978; Saiers and Hornberger, 1996; Flury et al.,
622 2004).

623 On the contrary, the influence of non-equilibrium sorption on reactive transport may be
624 critical for common hydrological conditions. In a porous medium of characteristic length L
625 (m) and humidity θ (-), a characteristic water flux density q_i (m³ s⁻¹ m⁻²) corresponds to a
626 water residence time:

$$T_w = \frac{q_i}{L \theta}$$

627 Sorption and desorption can generally be considered instantaneous for Damköhler numbers
628 $Da_1 = T_w/T^+$ and $Da_2 = T_w/T^-$ higher than 100 (e.g. Bahr and Rubin, 1987). For soils S and H,
629 sorption had very short half-lives T^+ (0.2 and 0.3 h) and can be considered much faster than
630 water residence time in a soil column for common hydrological situations. However,
631 desorption has much longer half-lives T^- (3 and 9 days) and may be often comparable to water
632 residence time. As a result, the equilibrium model K_d may be appropriate for very slow water
633 flows as observed in underground or deep geological nuclear waste repositories
634 (Grigaliūnienė et al., 2020; Medved' and Černý, 2019; Yim and Simonson, 2000). But non-
635 equilibrium model EK3 model seems better appropriate for the fast transient contamination

636 and infiltration conditions occurring in the unsaturated zone (Ardois and Szenknect, 2005;
 637 Brusseau et al., 1989; Maraqa et al., 1999; Testoni et al., 2017).



638

639 **Figure 6.** Applicability domains of the models K_d (linear), EK3 and EK5 at a given time t of a
 640 reactive transport scenario with mean residence time of water $T_w(t)$ and dissolved cesium
 641 concentration $C_w(t)$. This representation is specific to this study, where it was observed that
 642 type-2 sorption time T^+ was shorter than desorption time T^- , and that the density of type-2
 643 sorption sites (C_{s2}^{max}) was much lower than the density of type-1 sites (C_{s1}^{max}).

644 5. CONCLUSIONS

645 This work demonstrated that non-equilibrium and non-linear processes can influence
646 cesium sorption in conditions of reactive transport.

647 For each studied soil, the 4 stirred flow-through reactor experiments indicated that cesium
648 was less retarded when injected concentrations and/or flow rate increased. The proposed
649 sorption model EK5 reproduced significantly better the experimental observations compared
650 to simpler sorption models (K_d and EK3). It could well reproduce, with a single set of
651 parameters, the four breakthrough curves of cesium observed for both soils in the range 10-35
652 mL h⁻¹ for flow rate and 10⁻⁸-10⁻³ mol L⁻¹ for injection concentration. For both soils, the fitted
653 EK5 parameters suggested contrasted conditions of cesium sorption between equilibrium and
654 non-equilibrium sites. The equilibrium sites had a sorption capacity comparable to soil CEC,
655 but had a low affinity to cesium (40-60 L kg⁻¹). The non-equilibrium sites had a much shorter
656 sorption half-time (0.2-0.3 hours) compared to half-time of desorption (3-9 days), which
657 allows pseudo-irreversible cesium sorption at high flow rates. The non-equilibrium sites had a
658 strong affinity to cesium (3489-6171 L kg⁻¹) but their sorption capacity only represented 0.02-
659 0.04% of the CEC. The type-1 equilibrium and type-2 kinetic sites postulated by the EK5
660 model are an empirical representation of soil sorption sites that seems physically sound. They
661 seem to correspond respectively to ion-exchange and surface complexation sites of clay
662 minerals, as suggested by the similarity between their fitted and measured sorption capacities.

663 From a methodological standpoint, this study also showed that an experimental design
664 combining four flow-through reactor experiments with different conditions of flow rate and
665 injection concentration allows a precise identification of the 5 parameters of the proposed
666 EK5 model. This study also suggested the conditions of Cs reactive transport for which non-
667 equilibrium and nonlinear effects are important and thus variants of the EK5 model may be

668 more realistic than the K_d model. Non-equilibrium sorption effects increase when water
669 residence time decreases and becomes comparable to the half times of sorption and desorption
670 reactions (respectively 1 hour and 6-20 days for the studied soils). Non-linear sorption effects
671 emerge when sorbed Cs concentration is close to sorption capacity limits of type-2 and type-1
672 sites (approximately 1% and 99% of CEC for the studied soils). However, the applicability of
673 proposed EK model calibrated in the laboratory for predicting the reactor transport of Cs *in*
674 *situ* on contaminated soils has not been fully demonstrated yet. The validity and parameter
675 values of the EK5 model derived here from stirred flow-through reactor experiments concern
676 small representative elementary volumes and may no longer apply for complex flows in
677 porous media where other processes of nonlinear and non-equilibrium sorption may emerge.
678 Further experiments on soils with more contrasted physico-chemical properties (e.g. content
679 in clay minerals) and on systems of different levels of complexity (from batch reactors to soil
680 columns) are necessary to generalize the findings of this work.

681

682 **ACKNOWLEDGEMENTS**

683 This research was funded by Electricité de France (EDF) and IRSN in the framework of the
684 project GGP-Environnement (v1-300, 2017-2020).

685 **REFERENCES**

686 Antonopoulos-Domis M., Clouvas A., Hiladakis A., Kadi S., 1995. Radiocesium distribution
687 in undisturbed soil: measurements and diffusion-advection model. *Health Physics* 1995; 69:
688 949-953. <https://doi.org/10.1097/00004032-199512000-00009>.

689 Ardois C., Szenknect S., 2005. Capability of the Kd model to predict radionuclides behaviour
690 and transport in unsaturated columns under steady flow conditions. *Radioprotection* 40, S53–
691 S59. <https://doi.org/10.1051/radiopro:2005s1-009>. Vol 40, 2005.

692 Avery S.V., 1996. Fate of caesium in the environment: distribution between the abiotic and
693 biotic components of aquatic and terrestrial ecosystems. *Journal of Environmental*
694 *Radioactivity* 30: 139-171.

695 Bahr J.M., Rubin J., 1987. Direct comparison of kinetic and local equilibrium formulations
696 for solute transport affected by surface reactions. *Water Resources Research* 23: 438-452.

697 Bar- Tal A., Feigenbaum S., Sparks D.L., Pesek J.D., 1990. Analyses of Adsorption Kinetics
698 Using a Stirred- Flow Chamber: I. Theory and Critical Tests. *Soil Science Society of*
699 *America Journal* 54: 1273-1278.

700 Beale E.M.L., 1960. Confidence Regions in Non-Linear Estimation. *Journal of the Royal*
701 *Statistical Society. Series B (Methodological)* 22: 41-88.

702 Belsley D.A., Kuh E., Welsch R.E., 1980. *Regression diagnostics : identifying influential data*
703 *and sources of collinearity.* John Wiley and sons, Hoboken, New Jersey.
704 <http://doi.org/10.1002/0471725153>

705 Benedicto A., Missana T., Fernández A.M., 2014. Interlayer collapse affects on cesium
706 adsorption onto illite. *Environmental Science & Technology* 48: 4909-4915.

707 Bossew P., Kirchner G., 2004. Modelling the vertical distribution of radionuclides in soil. Part
708 1: the convection–dispersion equation revisited. *Journal of Environmental Radioactivity* 73:
709 127-150.

710 Bostick B.C., Vairavamurthy M.A., Karthikeyan K., Chorover J., 2002. Cesium adsorption on
711 clay minerals: An EXAFS spectroscopic investigation. *Environmental Science & Technology*
712 36: 2670-2676.

713 Bouzidi A., Souahi F., Hanini S., 2010. Sorption behavior of cesium on Ain Oussera soil
714 under different physicochemical conditions. *Journal of Hazardous Materials* 184: 640-646.

715 Bradbury M.H., Baeyens B., 2000. A generalised sorption model for the concentration
716 dependent uptake of caesium by argillaceous rocks. *Journal of Contaminant Hydrology* 42:
717 141-163.

718 Brouwer E., Baeyens B., Maes A., Cremers A., 1983. Cesium and rubidium ion equilibria
719 in illite clay. *The Journal of Physical Chemistry* 87: 1213-1219. Brun R., Reichert P., Künsch
720 H.R., 2001. Practical identifiability analysis of large environmental simulation models. *Water*
721 *Resources Research* 37: 1015-1030.

722 Brusseau M.L., Jessup R.E., Rao P.S.C., 1989. Modeling the transport of solutes influenced
723 by multiprocess nonequilibrium. *Water Resources Research* 25: 1971-1988.

724 Cameron D., Klute A., 1977. Convective- dispersive solute transport with a combined
725 equilibrium and kinetic adsorption model. *Water Resources Research* 13: 183-188.

726 Castrillejo M., Casacuberta N., Breier C.F., Pike S.M., Masqué P., Buesseler K.O., 2016.
727 Reassessment of ⁹⁰Sr, ¹³⁷Cs, and ¹³⁴Cs in the coast off Japan derived from the Fukushima
728 Dai-ichi nuclear accident. *Environmental Science & Technology* 50: 173-180.

729 Chaif H., Coppin F., Bahi A., Garcia-Sanchez L., 2021. Influence of non-equilibrium sorption
730 on the vertical migration of ¹³⁷Cs in forest mineral soils of Fukushima Prefecture. *Journal of*
731 *Environmental Radioactivity* 232: 106567.

732 Chen G.-N., Li Y.-C., Zuo X.-R., Ke H., Chen Y.-M., 2020. Comparison of Adsorption
733 Behaviors of Kaolin from Column and Batch Tests: Concept of Dual Porosity. *Journal of*
734 *Environmental Engineering* 146: 04020102.

735 Cherif M.A., 2017. Dynamic modeling of the (bio)availability of radionuclides in soils: a
736 comparative model-experiment approach applied to the transfer of Cs (I) in the rhizosphere
737 (in french). PhD thesis, Aix-Marseille Université, 2017.
738 <http://www.theses.fr/2017AIXM0547>.

739 Cherif M.A., Martin-Garin A., Gérard F., Bildstein O., 2017. A robust and parsimonious
740 model for caesium sorption on clay minerals and natural clay materials. *Applied*
741 *Geochemistry* 87: 22-37.

742 Chorover J., Choi S., Amistadi M.K., Karthikeyan K., Crosson G., Mueller K.T., 2003.
743 Linking cesium and strontium uptake to kaolinite weathering in simulated tank waste
744 leachate. *Environmental Science & Technology* 37: 2200-2208.

745 Comans R.N.J., Hockley D.E., 1992. Kinetics of cesium sorption on illite. *Geochimica et*
746 *Cosmochimica Acta* 56: 1157-1164.

747 Cornell R.M., 1993. Adsorption of cesium on minerals: A review. *Journal of Radioanalytical*
748 *and Nuclear Chemistry* 171: 483-500.

749 Durrant C.B., Begg J.D., Kersting A.B., Zavarin M., 2018. Cesium sorption reversibility and
750 kinetics on illite, montmorillonite, and kaolinite. *Science of The Total Environment* 610-611:
751 511-520.

752 Eberl D.D., 1980. Alkali cation selectivity and fixation by clay minerals. *Clays and clay*
753 *minerals* 28: 161-172.

754 Eliason J., 1966. Montmorillonite exchange equilibria with strontium-sodium-cesium.
755 *American Mineralogist: Journal of Earth and Planetary Materials* 51: 324-335.

756 Fesch C., Simon W., Haderlein S.B., Reichert P., Schwarzenbach R.P., 1998. Nonlinear
757 sorption and nonequilibrium solute transport in aggregated porous media: Experiments,
758 process identification and modeling. *Journal of Contaminant Hydrology* 31: 373-407.

759 Fiengo Perez F., Sweeck L., Bauwens W., Van Hees M., Elskens M., 2015. Adsorption and
760 desorption kinetics of ⁶⁰Co and ¹³⁷Cs in freshwater rivers. *Journal of Environmental*
761 *Radioactivity* 149:81-89. <https://doi.org/10.1016/j.jenvrad.2015.07.010>

762 Flury M., Czigány S., Chen G., Harsh J.B., 2004. Cesium migration in saturated silica sand
763 and Hanford sediments as impacted by ionic strength. *Journal of Contaminant Hydrology* 71:
764 111-126.

765 Francis C., Brinkley F., 1976. Preferential adsorption of ¹³⁷Cs to micaceous minerals in
766 contaminated freshwater sediment. *Nature* 260: 511-513.

767 Fukui M., 1978. Evaluation of a Combined Sorption Model for Describing Cesium Transport
768 in a Soil. *Health Physics* 35: 552-562.

769 Fuller A.J., Shaw S., Ward M.B., Haigh S.J., Mosselmans J.F.W., Peacock C.L., Stackhouse
770 S., Dent A.J., Trivedi D., Burke I.T., 2015. Caesium incorporation and retention in illite
771 interlayers. *Applied Clay Science* 108: 128-134.

772 Garcia-Sanchez L., Loffredo N., Mounier S., Martin-Garin A., Coppin F., 2014. Kinetics of
773 selenate sorption in soil as influenced by biotic and abiotic conditions: a stirred flow-through
774 reactor study. *Journal of Environmental Radioactivity* 138: 38-49.

775 Gil-García C., Rigol A., Vidal M., 2009. New best estimates for radionuclide solid–liquid
776 distribution coefficients in soils, Part 1: radiostrontium and radiocaesium. *Journal of*
777 *Environmental Radioactivity* 100: 690-696.

778 Grigaliūnienė D., Poškas R., Kilda R., Jouhara H., Poškas P., 2020. Modeling radionuclide
779 migration from activated metallic waste disposal in a generic geological repository in
780 Lithuania. *Nuclear Engineering and Design* 370: 110885.

781 Huet S., Bouvier A., Poursat M.-A., Jolivet E., 2004. Accuracy of estimators, confidence
782 intervals and tests. *Statistical Tools for Nonlinear Regression: A Practical Guide With S-*
783 *PLUS and R Examples*. Springer Verlag, New York. <https://doi.org/10.1007/b97288>.

784 IAEA, 2009. Quantification of Radionuclide Transfer in Terrestrial and Freshwater
785 Environments for Radiological Assessments. Report IAEA-TECDOC-1616. International
786 Atomic Energy Agency, Vienna.

787 Iliina S.M., Marang L., Lourino-Cabana B., Eyrolle F., Boyer P., Coppin F., Sivry Y. Gélabert
788 A., Benedetti M.F., 2020. Solid/liquid ratios of trace elements and radionuclides during a
789 Nuclear Power Plant liquid discharge in the Seine River: Field measurements vs geochemical
790 modeling. *Journal of Environmental Radioactivity* 220-221: 106317.

791 Jackson M., 1962. Interlayering of expansible layer silicates in soils by chemical weathering.
792 *Clays and clay minerals* 11: 29-46.

793 Jagercikova M., Cornu S., Le Bas C., Evrard O., 2015. Vertical distributions of ¹³⁷Cs in
794 soils: a meta-analysis. *Journal of Soils and Sediments* 15: 81-95.

795 Jarvis N.J., Taylor A., Larsbo M., Etana A., Rosén K., 2010. Modelling the effects of
796 bioturbation on the re-distribution of ¹³⁷Cs in an undisturbed grassland soil. *European*
797 *Journal of Soil Science* 61: 24-34.

798 Klement A.W. Jr, 1965. Radioactive fallout phenomena and mechanisms. *Health Physics* 11:
799 1265-1274.

800 Konoplev A, Bulgakov A, Hilton J, Comans R, Popov V., 1997. Long-term kinetics of
801 radiocesium fixation by soils. In: G. Desmet et al. (Eds), *Freshwater and Estuarine*
802 *Radioecology*, Elsevier, pp.173-182.

803 Kurikami H., Malins A., Takeishi M., Saito K., Iijima K., 2017. Coupling the advection-
804 dispersion equation with fully kinetic reversible/irreversible sorption terms to model
805 radiocesium soil profiles in Fukushima Prefecture. *Journal of Environmental Radioactivity*
806 171: 99-109.

807 Limousin G., Gaudet J.P., Charlet L., Szenknect S., Barthès V., Krimissa M., 2007. Sorption
808 isotherms: A review on physical bases, modeling and measurement. *Applied Geochemistry*
809 22: 249-275.

810 Maes A., Cremers A., 1986. Highly selective ion exchange in clay minerals and zeolites. In:
811 *Geochemical Processes at Mineral Surfaces*, Chapter 13, pp 254-295. ACS Symposium Series
812 Vol. 323. <https://doi.org/10.1021/bk-1987-0323.ch013>.

813 Maraqa M.A., Wallace R.B., Voice T.C., 1999. Effects of residence time and degree of water
814 saturation on sorption nonequilibrium parameters. *Journal of Contaminant Hydrology* 36: 53-
815 72.

816 Martin-Garin A., Van Cappellen P., Charlet L., 2003. Aqueous cadmium uptake by calcite: a
817 stirred flow-through reactor study. *Geochimica et Cosmochimica Acta* 67: 2763-2774.

818 Mazet P., 2008. Influence of transient flow on the mobility of strontium in unsaturated sand
819 columns (in french). PhD thesis, Université Joseph Fourier, Grenoble.

820 Medved' I., Černý R., 2019. Modeling of radionuclide transport in porous media: A review of
821 recent studies. *Journal of Nuclear Materials* 526: 151765.

822 Mishra S., Sahoo S.K., Bossew P., Sorimachi A., Tokonami S., 2018. Reprint of “Vertical
823 migration of radio-caesium derived from the Fukushima Dai-ichi Nuclear Power Plant
824 accident in undisturbed soils of grassland and forest?”. *Journal of Geochemical Exploration*
825 184: 271-295. <https://doi.org/10.1016/j.gexplo.2016.07.027>

826 Missana T., Benedicto A., García-Gutiérrez M., Alonso U., 2014a. Modeling cesium retention
827 onto Na-, K- and Ca-smectite: Effects of ionic strength, exchange and competing cations on
828 the determination of selectivity coefficients. *Geochimica et Cosmochimica Acta* 128: 266-
829 277.

830 Missana T., García-Gutiérrez M., Alonso U., 2004. Kinetics and irreversibility of cesium and
831 uranium sorption onto bentonite colloids in a deep granitic environment. *Applied Clay*
832 *Science* 26: 137-150.

833 Missana T., García-Gutiérrez M., Benedicto A., Ayora C., De-Pourcq K., 2014b. Modelling
834 of Cs sorption in natural mixed-clays and the effects of ion competition. *Applied*
835 *Geochemistry* 49: 95-102.

836 Montes M.L., Silva L.M.S., Sá C.S.A., Runco J., Taylor M.A., Desimoni J., 2013. Inventories
837 and concentration profiles of ¹³⁷Cs in undisturbed soils in the northeast of Buenos Aires
838 Province, Argentina. *Journal of Environmental Radioactivity* 116: 133-140.

839 Murota K., Saito T., Tanaka S., 2016. Desorption kinetics of cesium from Fukushima soils.
840 *Journal of Environmental Radioactivity* 153: 134-140.

841 Nakamaru Y., Ishikawa N., Tagami K., Uchida S., 2007. Role of soil organic matter in the
842 mobility of radiocesium in agricultural soils common in Japan. *Colloids and Surfaces A:
843 Physicochemical and Engineering Aspects* 306: 111-117.

844 Nicoulaud-Gouin V., Garcia-Sanchez L., Giacalone M., Attard J.C., Martin-Garin A., Bois
845 F.Y., 2016. Identifiability of sorption parameters in stirred flow-through reactor experiments
846 and their identification with a Bayesian approach. *Journal of Environmental Radioactivity*
847 162-163: 328-339.

848 Okumura M., Kerisit S., Bourg I.C., Lammers L.N., Ikeda T., Sassi M., Rosso K.M., Machida
849 M. 2019. Radiocesium interaction with clay minerals: Theory and simulation advances Post-
850 Fukushima. *Journal of Environmental Radioactivity* 89: 135-145.

851 Ota M., Nagai H., Koarashi J., 2016. Modeling dynamics of ¹³⁷Cs in forest surface
852 environments: Application to a contaminated forest site near Fukushima and assessment of
853 potential impacts of soil organic matter interactions. *Science of The Total Environment* 551-
854 552: 590-604.

855 Poinssot C., Baeyens B., Bradbury M.H., 1999. Experimental and modelling studies of
856 caesium sorption on illite. *Geochimica et Cosmochimica Acta* 63: 3217-3227.

857 Porro I., Newman M.E., Dunnivant F.M., 2000. Comparison of batch and column methods for
858 determining strontium distribution coefficients for unsaturated transport in basalt.
859 *Environmental Science & Technology* 34: 1679-1686.

860 R Core Team, 2021. R: A Language and Environment for Statistical Computing. R
861 Foundation for Statistical Computing, Vienna, Austria. <https://www.R-project.org/>

862 Rich C., Black W., 1964. Potassium exchange as affected by cation size, pH, and mineral
863 structure. *Soil Science* 97: 384-390.

864 Rigol A., Vidal M., Rauret G., 2002. An overview of the effect of organic matter on soil–
865 radiocaesium interaction: implications in root uptake. *Journal of Environmental Radioactivity*
866 58: 191-216.

867 Rosén K., Öborn I., Lönsjö H., 1999. Migration of radiocaesium in Swedish soil profiles after
868 the Chernobyl accident, 1987–1995. *Journal of Environmental Radioactivity* 46: 45-66.

869 Saiers J.E., Hornberger G.M., 1996. Migration of ¹³⁷Cs through quartz sand: experimental
870 results and modeling approaches. *Journal of Contaminant Hydrology* 22: 255-270.

871 Sardin M., Schweich D., Leij F.J., van Genuchten M.Th., 1991. Modeling the Nonequilibrium
872 Transport of Linearly Interacting Solutes in Porous Media: A Review. *Water Resources*
873 *Research* 27: 2287-2307.

874 Savoye S., Beaucaire C., Fayette A., Herbette M., Coelho D., 2012. Mobility of cesium
875 through the callovo-oxfordian claystones under partially saturated conditions. *Environmental*
876 *Science & Technology* 46: 2633-2641.

877 Sawhney B., 1972. Selective sorption and fixation of cations by clay minerals: a review.
878 *Clays and clay minerals* 20: 93-100.

879 Schnaar G., Brusseau M.L., 2014. Nonideal Transport of Contaminants in Heterogeneous
880 Porous Media: 11. Testing the Experiment Condition Dependency of the Continuous-
881 Distribution Rate Model for Sorption-Desorption. *Water, Air and Soil Pollution* 225: 2136.

882 Schwertmann U., Taylor R.M., 1989. Iron oxides. In: Dixon, J.B. and Weed S.B. (Eds.),
883 *Minerals in Soil Environments*, 2nd Edition, Soil Science Society of America, Inc., Madison,
884 pp.379-438. <https://doi.org/10.2136/sssabookser1.2ed.c8>.

885 Seber G.A.F., Wild C.J., 1989. Nonlinear regression. John Wiley, New York.
886 <https://doi.org/10.1002/0471725315>.

887 Selim H., Mansell R., 1976. Analytical solution of the equation for transport of reactive
888 solutes through soils. *Water Resources Research* 12: 528-532.

889 Selim, H.M., Davidson J.M., Mansell R.S., 1976. Evaluation of a two-site adsorption–
890 desorption model for describing solute transport in soil. p. 444–448. In *Proc. Summer*
891 *Computer Simulation Conf.*, Washington, DC. 12–14 July 1976. Simulation Councils, La
892 Jolla, CA.

893 Shenber M., Eriksson Å., 1993. Sorption behaviour of caesium in various soils. *Journal of*
894 *Environmental Radioactivity* 19: 41-51.

895 Siroux B., 2017. Interactions in a cesium, strontium/natural organic matter and soil clays
896 system. From decontamination to remediation (in french). PhD thesis. Université Sorbonne
897 Paris Cité. <https://tel.archives-ouvertes.fr/tel-02083966>

898 Siroux B., Latrille C., Beaucaire C., Petcut C., Tabarant M., Benedetti M.F., Reiller P.E.,
899 2021. On the use of a multi-site ion-exchange model to predictively simulate the adsorption
900 behaviour of strontium and caesium onto French agricultural soils, *Applied Geochemistry*
901 132, 105052. <https://doi.org/10.1016/j.apgeochem.2021.105052>.

902 Sparks D., Zelazny L., Martens D., 1980. Kinetics of potassium desorption in soil using
903 miscible displacement. *Soil Science Society of America Journal* 44: 1205-1208.

904 Sposito G., 1984. *The surface chemistry of soils*. Oxford University Press, New York.

905 Staunton S., Roubaud M., 1997. Adsorption of ¹³⁷ Cs on montmorillonite and illite: effect of
906 charge compensating cation, ionic strength, concentration of Cs, K and fulvic acid. *Clays and*
907 *clay minerals* 45: 251-260.

908 Steinhauser G., Niisoe T., Harada K.H., Shozugawa K., Schneider S., Synal H.-A., Walther
909 C., Christl M., Nanba K., Ishikawa H., Koizumi A., 2015. Post-accident sporadic releases of
910 airborne radionuclides from the Fukushima Daiichi nuclear power plant site. *Environmental*
911 *Science & Technology* 49: 14028-14035.

912 Stewart G.W., 1987. Collinearity and least squares regression (with discussion). *Statistical*
913 *Science* 2: 68-100.

914 Strebl F., Gerzabek M., Bossew P., Kienzl K., 1999 Distribution of radiocaesium in an
915 Austrian forest stand. *Science of The Total Environment* 226: 75-83.

916 Szenknect S., 2003. Radionuclides migration in the unsaturated zone: experimental study and
917 modeling applied to the Chernobyl pilot site (in french). PhD thesis. Université Joseph
918 Fourier, Grenoble.

919 Szenknect S., Gaudet J.-P., Dewiere L., 2003. Evaluation of distribution coefficients for the
920 prediction of strontium and cesium migration in a natural sand at different water contents.
921 *Journal de Physique IV (Proceedings)* 107(1): 1279-1282.
922 <https://doi.org/10.1051/jp4:20020534>

923 Takahashi J., Onda Y., Hihara D., Tamura K., 2019. Six-year monitoring of the vertical
924 distribution of radiocesium in three forest soils after the Fukushima Dai-ichi Nuclear Power
925 Plant accident. *Journal of Environmental Radioactivity* 210: 105811.

926 Testoni R., Levizzari R., De Salve M., 2017. Coupling of unsaturated zone and saturated zone
927 in radionuclide transport simulations. *Progress in Nuclear Energy* 95: 84-95.

928 Toro J., Padilla I.Y., 2017. Spatial Distribution of Fate and Transport Parameters Using
929 CXTFIT in a Karstified Limestone Model. American Geophysical Union, Fall Meeting 2017,
930 abstract H51C-1288.

931 Toso J., Velasco R., 2001. Describing the observed vertical transport of radiocesium in
932 specific soils with three time-dependent models. *Journal of Environmental Radioactivity* 53:
933 133-144.

934 Soetaert, K., Petzoldt, T., Setzer, R.W., 2010. Solving differential equations in R: package
935 deSolve. *J. Stat. Software* 33 (9), 1-25. <https://doi.org/10.18637/JSS.V033.I09>.

936 Valcke E., Cremers A., 1994. Sorption-desorption dynamics of radiocaesium in organic
937 matter soils. *Science of The Total Environment* 157: 275-283.

938 Van Cappellen P., Qiu, L., 1997a. Biogenic silica dissolution in sediments of the Southern
939 Ocean. I. Solubility. *Deep-Sea Res. Part II* 1997; 44: 1109-1128.

940 Van Cappellen P., Qiu L., 1997b. Biogenic silica dissolution in sediments of the Southern
941 Ocean. II. Kinetics. *Deep Sea Research Part II: Topical Studies in Oceanography* 1997; 44:
942 1129-1149.

943 van Genuchten M.Th., Simunek J.J., Leij F.J., Toride N., Šejna M., 2012. STANMOD: Model
944 Use, Calibration, and Validation. *Transactions of the ASAE* 55:1353-1366.
945 <https://doi.org/10.13031/2013.42247>.

946 van Genuchten M.Th., Wagenet R.J., 1989. Two-Site/Two-Region Models for Pesticide
947 Transport and Degradation: Theoretical Development and Analytical Solutions. *Soil Science*
948 *Society of America Journal* 53: 1303-1310.

949 Wahlberg J., Fishman M.J., 1962. Adsorption of cesium on clay minerals. Geological Survey
950 Bulletin 1140-A, US Government Printing Office. <https://doi.org/10.3133/b1140A>.

951 Wang W.-Z., Brusseau M.L., Artiola J.F., 1998. Nonequilibrium and nonlinear sorption
952 during transport of cadmium, nickel, and strontium through subsurface soils. In: Jenne E.A.
953 (Ed.), Adsorption of Metals by Geomedia, Academic Press, pp. 427-443.
954 <https://doi.org/10.1016/B978-012384245-9/50021-9>.

955 Wendling L.A., Harsh J.B., Ward T.E., Palmer C.D., Hamilton M.A., Boyle J.S., Flury M.,
956 2005. Cesium desorption from illite as affected by exudates from rhizosphere bacteria.
957 Environmental Science & Technology 39: 4505-4512.

958 Yim M.-S., Simonson S.A., 2000. Performance assessment models for low level radioactive
959 waste disposal facilities: A review. Progress in Nuclear Energy 36: 1-38.

960 Zachara J.M., Smith S.C., Liu C., McKinley J.P., Serne R.J., Gassman P.L., 2002. Sorption of
961 Cs⁺ to micaceous subsurface sediments from the Hanford site, USA. Geochimica et
962 Cosmochimica Acta 66: 193-211.